Co$_3$O$_4$-based catalysts for propane total oxidation: A state-of-the-art minireview

Weidong Zhang [a,b], Jose Luis Valverde [c], Anne Giroir-Fendler [b,*]

[a] School of Chemistry and Chemical Engineering, Anhui Province Key Laboratory of Coal Clean Conversion and High Valued Utilization, Anhui University of Technology, Ma'anshan 243002, China
[b] Univ. Lyon, Université Claude Bernard Lyon 1, CNRS, IRCELYON, 2 Avenue Albert Einstein, Villeurbanne F-69622, France
[c] Faculty of Chemical Science and Technology, University of Castilla-La Mancha, Avenida Camilo José Cela 12, 13005 Ciudad Real, Spain

ARTICLE INFO

ABSTRACT

Co$_3$O$_4$-based catalysts are promising systems for volatile organic compounds (VOCs) elimination. In the last few years, significant efforts have been devoted to improving their catalytic activity at low temperatures. This review summarizes recent progress on single, composite, and supported Co$_3$O$_4$ catalysts for the total oxidation of propane, a representative VOC. First, single Co$_3$O$_4$ modification is comprehensively discussed, including optimization of synthesis parameters, structure construction, morphology control, facet engineering, and defect engineering, with the aim of tuning surface-active species. Secondly, the design and construction of composite Co$_3$O$_4$ are presented in detail, which could produce synergetic effects such as electronic, geometric, and interfacial effects that promote catalytic performance. Thirdly, supported Co$_3$O$_4$ systems desirable in industrial applications are introduced. Moreover, the propane total oxidation mechanisms over Co$_3$O$_4$-based catalysts are summarized. Some poisoning effects on propane oxidation over Co$_3$O$_4$-based catalysts are also discussed. Finally, the challenges, opportunities, and future research direction of developing advanced Co$_3$O$_4$-based catalysts are prospected.

1. Introduction

Volatile organic compounds (VOCs) in the atmosphere, mainly from petroleum refining, chemical manufacture, paper production, paint drying, and textile manufacture [1–3], have caused serious environmental problems, e.g. the damage of stratospheric ozone [4], the formation of ground-level ozone and secondary aerosol [2], the formation of photochemical smog through reactions with other atmospheric pollutants such as NO$_x$ and SO$_x$ [2], and the enhanced global warming by absorbing solar or terrestrial infrared radiation [5]. On the other hand, due to their toxicity, high stability, and persistence in the environment, some VOCs may threaten human health and cause irreversible damage after long-time exposure [3,5]. Therefore, it is urgent and necessary to control VOCs emissions to protect the environment and human health. Catalytic oxidation is one of the most effective and promising VOCs abatement techniques. The key subject in catalytic oxidation is the development of highly active, selective, and long-life catalysts. Up to now, numerous catalytic materials have been developed, which can be divided into two main types, noble metals (Pt, Pd, Au, etc.) and

non-noble metal oxides (Mn, Fe, Co, Ni, Cu, Ce oxides, etc.). Noble metal catalysts are generally more efficient at lowering the activation energy than metal oxide catalysts. However, their scarcity, high cost, and sintering issues urge researchers to develop more economic alternatives. Among the most investigated metal oxide catalysts, Co$_3$O$_4$ stands out and is extensively studied due to its unique physicochemical properties, good redox ability, and superior activity [6]. Co$_3$O$_4$-based catalysts have been reported in the catalytic oxidation of CO [7,8], CH$_4$ [8], and various types of VOCs, including alkanes (ethane [9], propane [10–67], butane [68], hexane [69]), alkenes (ethene [70,71], propene [72,73]), aromatic hydrocarbons (benzene [74], toluene [75–81], o-xylene [82,83], naphthalene [66]), oxygen-containing VOCs (methanol [84], formaldehyde [85–87], ethanol [88], ethyl acetate [89], 2-propanol [90], acetone [91,92]), and halogenated VOCs (dichloromethane [93], 1,2-dichloroethane [4,94], vinyl chloride [95,96], dibromomethane [97,98]). Among these VOCs, propane is a representative alkane emitted from petrochemical processes and the main component of automobile exhaust, which is rather challenging to eliminate owing to its stable saturated C–H bond and is commonly used as a model pollutant for

catalyst performance evaluation. Co_3O_4 is one of the most promising catalysts for propane total oxidation. In some cases, the propane oxidation activity of Co_3O_4 is comparable to or even superior to noble metal catalysts [16,34,55,64]. In recent years, many encouraging advances in Co_3O_4-based catalysts for propane total oxidation have been achieved. There have been some latest reviews on the topic of VOCs oxidation in terms of pollutant sorts and sources [1,2], layered double hydroxides derived mixed metal oxides [99], manganese-based oxide catalysts [100], and oxygen vacancies [101]. Moreover, Liotta et al. provided in 2013 a systematic review on single and composite Co_3O_4 catalysts for low-temperature CO, CH_4, and VOCs oxidation. However, no specific review summarizing the comprehensive advances of Co_3O_4-based catalysts for propane total oxidation has been reported until now. Herein, we discuss this topic in the following aspects: i) single Co_3O_4 modification; ii) composite Co_3O_4 construction; iii) supported Co_3O_4 fabrication; iv) propane oxidation mechanism; v) poisoning effect on propane total oxidation; vi) future opportunities and challenges. Hopefully, this review will attract attention and boost the rational design of highly active and stable Co_3O_4-based catalysts for low-temperature propane total oxidation.

2. Structure, properties, and catalytic performance of Co_3O_4

Co_3O_4 is the most thermodynamically stable phase of cobalt oxide. Generally, Co_3O_4 does not decompose into CoO until it exceeds 850 °C [102]. It is a magnetic p-type semiconductor and has a cubic spinel structure with a lattice constant of 0.8084 nm. In a unit cell of Co_3O_4, Co^{2+} occupies 1/8 of tetrahedral voids and is coordinated with four lattice oxygen, Co^{3+} occupies 1/2 of octahedral voids and is coordinated with six lattice oxygen, and O^{2-} is cubic close-packed [103] (Fig. 1). The oxidation states and coordination environments of Co ions greatly affect the catalytic oxidation ability of Co_3O_4 [103]. Co_3O_4 exhibits weak strength of Co–O bond, low formation energy of oxygen vacancy, and high lattice oxygen transfer ability, which is favorable for total oxidation reactions [75]. In addition, owing to the unfilled d6 orbital of Co^{3+} and d7 orbital of Co^{2+}, Co_3O_4 shows high activity on the activation of the C–H bond via direct interaction between σ/σ * C–H orbitals with Dd-type-type orbitals [6]. Therefore, Co_3O_4 is highly active for propane oxidation, in which the breaking of C–H is the rate-determining step [11]. Table 1 summarizes the catalytic performance of recently reported Co_3O_4-based catalysts for propane total oxidation. The T_{90} (temperature corresponds to 90% propane conversion) values range from 170 °C to 372 °C. Most Co_3O_4-based catalysts can achieve 90% propane conversion at temperatures lower than 300 °C, demonstrating the superior propane total oxidation ability of Co_3O_4. The lowest T_{90} over single, composite, and supported Co_3O_4 catalysts are 170, 194, and 220 °C, respectively. Due to the variety of testing conditions including inlet propane concentration (0.1%−1%), oxygen concentration (2%−21%), weight hourly space velocity (WHSV, 9990−300,000 mL h^{-1} g^{-1}), as well as cobalt loading for supported Co_3O_4, it is difficult to compare the intrinsic propane oxidation activity of different systems. In the following
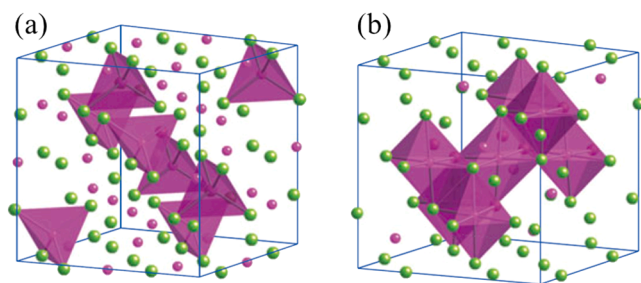

Fig. 1. Spinel structure of Co_3O_4: (a) Co^{2+} in tetrahedral environment and (b) Co^{3+} in octahedral environment. Green spheres = O^{2-}, purple spheres = Co^{2+}/Co^{3+} [104].

Table 1
Survey of propane total oxidation over Co_3O_4-based catalysts.

	Catalyst	Reactant composition	WHSV (mL h^{-1} g^{-1})	T_{90} (°C)	Ref.
Single Co_3O_4	Co-SAS 10% water	0.5% C_3H_8 + 20% O_2	15,000	200	[55]
	Co_3O_4-SD-250	0.4% C_3H_8 + 20% O_2	117,600	215	[64]
	CoNP	0.1% C_3H_8 + 21% O_2	120,000	246	[67]
	CoDP	0.1% C_3H_8 + 21% O_2	120,000	225	[13]
	Co-200	0.1% C_3H_8 + 21% O_2	30,000	170	[49]
	Co-CO_3	0.1% C_3H_8 + 21% O_2	40,000	226	[30]
	Co-9.5-HNO_3 treated	0.1% C_3H_8 + 21% O_2	40,000	211	[43]
	Co-CA	0.3% C_3H_8 + 21% O_2	30,000	250	[32]
	Co-PDO	0.3% C_3H_8 + 21% O_2	30,000	227	[38]
	C100–550	0.8% C_3H_8 + 20% O_2	120,000	213	[33]
	Mic-Co_3O_4	0.8% C_3H_8 + 21% O_2	120,000	372	[37]
	Co_3O_4-30	1% C_3H_8 + 20% O_2	300,000	228	[52]
	Co_3O_4-S	0.9% C_3H_8 + 21% O_2	30,000	208	[24]
	Co_3O_4-B	0.2% C_3H_8 + 5% O_2	120,000	278	[47]
	Co_3O_4-H	1.0% C_3H_8 + 10% O_2	9990	239	[20]
	Co_3O_4-R	0.25% C_3H_8 + 21% O_2	12,000 (h^{-1})	195	[45]
	Co_3O_4-110	0.5% C_3H_8 + 10% O_2	60,000	218	[63]
	Co_3O_4-350	1% C_3H_8 + 10% O_2	60,000	275	[58]
	Co_3O_4-P	0.2% C_3H_8 + 2.5% O_2	18,000	186	[62]
	Co_3O_4-GC-6	1% C_3H_8 + 10% O_2	30,000	222	[22]
	Co_3O_4-AC	0.3% C_3H_8 + 10% O_2	240,000	250	[16]
	CoLa-1.8	1% C_3H_8 + 10% O_2	10,000	264	[46]
	Ca-Co_3O_4-Ac	0.2% C_3H_8 + 5% O_2	120,000	260	[57]
	Cu-Co_3O_4-110–3	0.5% C_3H_8 + 10% O_2	60,000	203	[63]
	$Mn_{0.05}$Co	0.1% C_3H_8 + 21% O_2	40,000	227	[31]
	1%Zr-Co_3O_4	0.1% C_3H_8 + 21% O_2	40,000	241	[50]
	1%Y-Co	0.1% C_3H_8 + 21% O_2	40,000	242	[54]
	Co_3O_4	0.25% C_3H_8 + 10% O_2	120,000	241	[19]
	Co-pH 8.5–1	0.1% C_3H_8 + 21% O_2	40,000	238	[25]
	Co-CO_3-3 T	0.1% C_3H_8 + 21% O_2	40,000	236	[26]
	Co_3O_4	0.1% C_3H_8 + 10% O_2	240,000	251	[34]
Composite Co_3O_4	CeCo30	1% C_3H_8 + 10% O_2	10,000	223	[11]
	Co_1Ce_1	0.6% C_3H_8 + 20% O_2	60,000	238	[17]
	$Co_2Ce_1O_x$	0.08% C_3H_8 + 10% O_2	90,000	249	[18]
	CoCeO$_x$-70	0.2% C_3H_8 + 5% O_2	120,000	310	[35]
	CeO_2 @Co_3O_4	0.8% C_3H_8 + 20% O_2	120,000	325	[39]

Table 1 (*continued*)

	Catalyst	Reactant composition	WHSV (mL h^{-1} g^{-1})	T_{90} (°C)	Ref.
	NiO-Co(0.3)	0.1% C_3H_8 + 18% O_2	30,000	236	[15]
	D-NiCo$_2$O$_4$	0.5% C_3H_8 + 10% O_2	60,000	194	[59]
	Co$_{2.3}$Mn$_{0.7}$O$_4$	0.4% C_3H_8 + 20% O_2	117,360	225	[12]
	Co$_2$Mn$_1$O$_6$	0.8% C_3H_8 + 20% O_2	12,000	225	[29]
	Co$_1$Mn$_3$O$_x$	0.2% C_3H_8 + 2.5% O_2	18,000	207	[41]
	1Co2Cr	0.2% C_3H_8 + 2% O_2	80,000	275	[36]
	Co$_4$Zr$_1$	0.2% C_3H_8 + 5% O_2	60,000	242	[56]
	LCO-AH	1% C_3H_8 + 10% O_2	100,000	312	[23]
	N-CoAlO/4 h	0.8% C_3H_8 + 20% O_2	120,000	266	[61]
Supported Co$_3$O$_4$	50%Co$_3$O$_4$/α-Al$_2$O$_3$	0.8% C_3H_8 + 20% O_2	120,000	284	[10]
	10CoAl-500RO	0.1% C_3H_8 + 18% O_2	30,000	247	[28]
	25Co$_3$O$_4$/ZSM-5-A	0.2% C_3H_8 + 2% O_2	80,000	281	[51]
	Co/ZSM-5 HT	0.2% C_3H_8 + 2% O_2	30,000	287	[44]
	CoO$_x$(5)/SiO$_2$	0.1% C_3H_8 + 8% O_2	30,000	323	[66]
	CoAO-450	0.1% C_3H_8 + 21% O_2	120,000	277	[14]
	Co-SBA-15	0.1% C_3H_8 + 21% O_2	6000 (h^{-1})	307	[21]
	Co/SiO$_2$ −N	0.2% C_3H_8 + 2.5% O_2	20,000	220	[40]
	2Fe−Co/HLS	0.2% C_3H_8 + 2.5% O_2	20,000	286	[60]
	10%Co/MCM-22(50)-A	0.1% C_3H_8 + 21% O_2	60,000	295	[48]

sections, the catalytic performance of the Co$_3$O$_4$-based catalysts is discussed in the sequence of single, composite, and supported CoO$_x$ catalysts.

3. Single Co$_3$O$_4$ for propane total oxidation

3.1. Synthesis parameters optimization

There are many methods developed for the preparation of single Co$_3$O$_4$ catalysts, including precipitation, hydrothermal/solvothermal synthesis, hard template route, solid-state reaction, sol-gel method, solution combustion synthesis, etc. The properties of single Co$_3$O$_4$ catalysts are highly dependent on the preparation parameters. To achieve satisfying catalytic performance of Co$_3$O$_4$, it is important to optimize the preparation parameters. Precipitation is a simple method using cheap chemicals and equipment, requiring neither costly surfactants nor harsh conditions, showing advantages of low energy consumption and scalable production, which is desirable for industrial applications. Taking the classic precipitation route as an example, one can see that there are many variables that affect the nature of the precipitate and accordingly the final catalyst (Fig. 2). Therefore, it is valuable to study and understand the roles of various factors in the preparation process, in order to establish an effective approach for rational synthesis of efficient Co$_3$O$_4$ catalysts.

Marin et al. prepared Co$_3$O$_4$ catalysts by a supercritical CO$_2$ antisolvent precipitation route and probed the effect of co-solvent water content and calcination temperature [55]. The optimal catalyst was obtained using 10 vol% co-solvent water and calcinating at 250 °C, which converted 50% propane at 175 °C, much better than the commercial 5 wt% Pt/Al$_2$O$_3$ benchmark catalyst. Nevertheless, this method using costly supercritical CO$_2$ is not favorable for practical application. Salek et al. synthesized porous Co$_3$O$_4$ catalysts using LiOH as precipitate and cobalt sulfate or nitrate as precursors [64]. They found that the catalyst derived from sulfate precursor was more active than that made from nitrate for propane oxidation, probably due to the enhanced surface acidity by the presence of sulfate groups. Zhang et al. obtained Co$_3$O$_4$ crystallites by adding ammonia to the freshly prepared cobalt hydroxide and subsequent calcination [67]. The ammonia-etched Co$_3$O$_4$ catalyst exhibited much smaller grain sizes, better reducibility, and more reactive surface oxygen species than the conventional precipitated one and thus enhanced propane oxidation activity. In their following work, they proposed a dispersion–precipitation route to synthesize nanosized Co$_3$O$_4$ catalysts, which included the formation of a CoO$_x$·H$_2$O colloidal system through the reaction of Co(OH)$_x$ and acetic acid, as well as dilution of the colloidal system to precipitate CoO$_x$·H$_2$O crystallite [13]. The nanosized Co$_3$O$_4$ outperformed the traditional Co$_3$O$_4$ in propane oxidation and is highly stable in a 76-h continuous test. Wang et al.
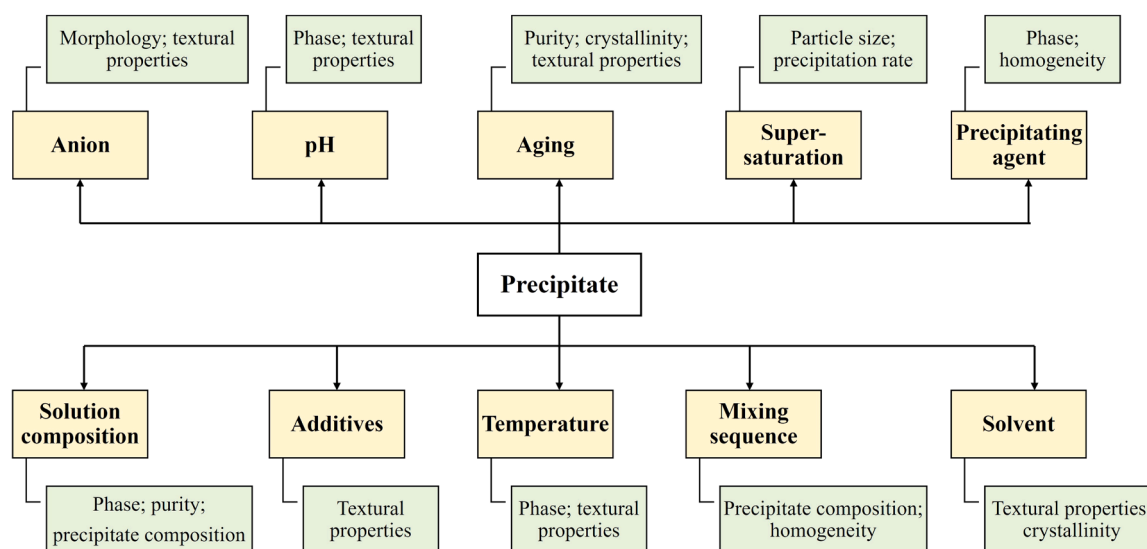

Fig. 2. Possible effect of precipitation variables on the properties of the precipitate.

prepared a series of Co_3O_4 catalysts by a hydrothermal method and investigated the effect of calcination temperature on their propane oxidation performance [49]. They found that the oxygen vacancy contents in Co_3O_4 gradually decreased with increasing the calcination temperature from 200 °C to 450 °C. The Co_3O_4 catalyst calcined at 200 °C exhibited a large surface area of 176 $m^2 \ g^{-1}$, excellent reducibility, and a high quantity of oxygen vacancies, thus demonstrated the best propane oxidation performance (T_{90} = 170 °C). Despite the excellent performance, Co_3O_4 catalysts calcined at such a low temperature still encounter sintering issues when applied at high temperature conditions.

Recently, our group made some efforts in optimizing Co_3O_4 nano-catalysts prepared via precipitation [30,43]. First, a set of Co_3O_4 catalysts using $H_2C_2O_4$, NaOH, Na_2CO_3, NH_4OH, and urea as precipitants were prepared and the effect of precipitation agent nature on the physicochemical properties and the catalytic performance of Co_3O_4 catalysts was probed [30]. The Na_2CO_3 precipitated Co_3O_4 catalyst showed the best performance for propane combustion (T_{90} = 226 °C), which was associated with the highly strained nanocrystalline structure, high content of surface Co^{2+}, and good low-temperature reducibility. In our follow-up work, the impact of precipitation pH on the physicochemical properties of the Co_3O_4 catalysts derived from sodium carbonate precipitation was studied [43]. The precipitation pH value was decisive in the composition of the cobalt precursors ($Co(OH)_x(CO_3)_{0.5}$ $_{(2-x)}•nH_2O$). The higher pH, the higher content of OH^- and H_2O in the basic cobalt carbonate. Co_3O_4 prepared at pH 9.5 exhibited the highest surface area, the largest number of defects, and the best reducibility. After treating with HNO_3, this catalyst can convert 90% of propane to CO_2 at 211 °C.

Liu et al. prepared three different Co_3O_4 catalysts using citric acid, oxalic acid, and tartaric acid as complexing agent, respectively [32]. They found that the type of carboxylic acids affected the distance between Co^{2+} in the precursor, which resulted in different crystallite size and specific surface area of the Co_3O_4 crystalline. The Co_3O_4 catalyst prepared from cobalt citrate precursor showed the best propane oxidation activity (T_{90} = 250 °C), owing to the best reducibility and the largest quantity of surface oxygen species. Following this study, they further explored the effect of C_2–C_5 diols introduction during the citric acid complexation process on the Co_3O_4 structure and propane oxidation activity [38]. They found that introducing diols resulted in the formation of CoO-Co_3O_4 mixed oxides with much smaller crystallite sizes and larger surface areas compared with reference Co_3O_4. The CoO-Co_3O_4 mixed oxides possessed weak Co–O bond strength, abundant active oxygen species, excellent redox ability, and thus superior propane elimination efficiency. Introducing 1,3-propanediol gave the best-performing CoO_x catalysts (T_{90} = 227 °C), which could maintain its activity even in the presence of H_2O. It should be noted that NO_x emissions occur during the decomposition of the catalyst precursor in this method, which is not conducive to scalable manufacturing in practical applications.

3.2. Structure construction

Constructing porous Co_3O_4 structure can benefit propane oxidation via the following aspects: i) boosting the adsorption and mass transfer of propane; ii) increasing the exposure of active site; iii) facilitating the formation of surface defects and oxygen vacancies. Garcia et al. fabricated various ordered Co_3O_4 materials (S_{BET} = 112 −173 $m^2 \ g^{-1}$) using mesoporous KIT-6 silica as a hard template and tested their performance in propane oxidation [33]. The results showed that the propane oxidation activity of the mesoporous Co_3O_4 is one order of magnitude higher than the one prepared by a precipitation method. The better activity of mesoporous Co_3O_4 is independent of the ordered structure but related to the large surface area and abundant oxygen vacancies. Considering that the mesoporous Co_3O_4 catalysts derived from hard-template did not undergo a calcination process, attention should be paid to the stability of

their pore structures. Lin et al. constructed Co_3O_4 nanoparticles-assembled microrods by the decomposition of metal-organic framework (MOF) and compared their performance with Co_3O_4 nanoparticles in propane total oxidation [37]. The MOF-derived Co_3O_4 showed higher activity than conventional Co_3O_4, due to a weak Co–O bond and a larger concentration of active oxygen species. Chen et al. fabricated ZIF-67-derived Co_3O_4 hollow cages using a bifunctional etching strategy, in which cobalt nitrate acted as both etchant of ZIFs and cobalt source [52]. The optimal Co_3O_4 hollow cages (etched by 30 g/L of cobalt nitrate in ethanol) can achieve full conversion of propane at 240 °C and maintain this performance at a space velocity up to 300,000 mL h^{-1} g^{-1}. This is a surprising progress since the catalytic performance of most Co_3O_4-based catalysts decreases with increasing WHSV due to the shortened contact time of reactants with the catalysts. The excellent propane oxidation activity benefited from the mesoporous structure, good redox properties, and plenty of surface-adsorbed oxygen.

3.3. Morphology control

By controlling the morphology of Co_3O_4, one can tune the surface cobalt species and oxygen coordination environment, which may in turn influence the activity of Co_3O_4. Chen et al. prepared Co_3O_4 nanocubes, nanosheets, and nanooctahedra via the hydrothermal method and molten salt method for the complete oxidation of propane [24]. They found that the Co^{2+} content attached by hydroxyl groups on Co_3O_4 decreased in the order of nanosheets > nanocubes > nanooctahedra, which agrees with their propane oxidation activity order. The Co_3O_4 nanosheets with abundant hydroxyl groups showed the best catalytic activity (T_{100} = 210 °C). The surface hydroxyl groups on Co_3O_4 nanosheets could change the propane oxidation pathway and thus boost its catalytic activity. Using a hydrothermal self-assembly strategy, Zhu et al. controllably fabricated hierarchical Co_3O_4 with ellipsoidal, flowerlike, book-shaped, and spindle-like morphologies and examined their performance in propane total oxidation [47]. Among the synthesized catalysts, book-shaped Co_3O_4-B had the best propane oxidation performance (T_{90} = 278 °C). The large surface area, highly reducible Co^{3+}, and high mobility of lattice oxygen of Co_3O_4-B made it an excellent propane oxidation catalyst.

3.4. Facet engineering

Co_3O_4 crystalline with specifically exposed crystal facets can have unique physicochemical properties, adsorption performance, and surface-active sites due to the preferentially exposed atoms and twisted electronic structures, which heavily affect the propane oxidation activity of Co_3O_4. Since Xie et al. reported that Co_3O_4 nanorods with predominantly exposed {110} planes favored the exposure of surface active Co^{3+} species for low-temperature CO oxidation [105], much attention has been attracted to the controllable synthesis of Co_3O_4 with highly active facets exposed [80,106–108]. By using a hydrothermal method, Yao et al. fabricated four different Co_3O_4 catalysts which mainly exposed {100}, {111}, {110}, and {112} facets and test their activity in propane combustion [20]. The activity follows the order of {111} > {100} > {110} > {112}. The best activity of hexagonal nanoplate Co_3O_4 catalysts with {111} facets could be attributed to the easy activation of C−H on Co_3O_4 {111} facets, as well as the high mobility of lattice oxygen and facile activation of gas phase oxygen. On the other hand, Jian et al. adopted a simple solvothermal strategy to synthesize rod-, sheet-, and cube-shaped Co_3O_4 with dominantly exposed {110}, {111}, and {100} facets, respectively [45]. The rod-like Co_3O_4 exposing {110} planes exhibited better activity (T_{90} = 195 °C) than that exposing {111} and {100} facets, due to the presence of large numbers of lattice defects, oxygen vacancies, and low-coordinated Co atoms. Similarly, Sun et al. demonstrated that {110} facet exposed Co_3O_4 catalyst was the best-performing one for propane total oxidation among Co_3O_4 catalysts with {112}, {111} and {100} facet exposed [63]. Li et al. obtained a

range of hexagonal layered Co_3O_4 catalysts by annealing the cobalt-based MOF at different temperatures [58]. The Co_3O_4 catalyst calcined at 350 °C with preferentially exposed {112} facets showed the best propane oxidation performance ($T_{90} = 275$ °C), much superior to that of the Co_3O_4 flakes with dominantly exposed {111} facets, which can be ascribed to its large specific surface area, rich oxygen defects, and good redox capacity. Li et al. fabricated particle-, sheet-, and rod-like Co_3O_4 for propane total oxidation [62]. They found that Co_3O_4 particle with predominantly exposed {110} plane was the most active one in propane oxidation while Co_3O_4 rod with predominantly exposed {111} plane exhibited the best water resistance. The presence of abundant surface reactive lattice oxygen species in Co_3O_4 particle with the {110} plane is the reason for its high activity, while the weak water adsorption capacity of Co_3O_4 rod with the {111} plane explains its excellent water tolerance. The above examples suggest that in most cases, exposing {110} planes could be beneficial for propane total oxidation over Co_3O_4 catalysts.

Bae et al. found that Mn doping behavior can also be determined by the exposed facets of the host Co_3O_4 [42]. As displayed in Fig. 3, 1%Mn could be successfully doped into Co_3O_4 cubes with {100} facets, but not into the lattice of Co_3O_4 octahedra with {111} facets. Instead, Mn was deposited and accumulated on the {111} facets of Co_3O_4 octahedra, causing the collapsed of octahedra and the formation of spherical particles. 1%Mn doping into Co_3O_4 cubes could increase the quantity and mobility of surface oxygen species, weaken the adsorption strength of oxygen on Co_3O_4 cubes, and thus give superior activity in the simultaneous oxidation of CO, propene, and propane with H_2O.

3.5. Defect engineering

Defect engineering is an effective way to regulate the physicochemical properties of Co_3O_4 by changing the surface charge distribution and lowering the coordination number. Defects in Co_3O_4 can cause electron delocalization of the Co−O bonds, reduce the formation energy of oxygen vacancy, boost the activation of oxygen species, and may offer adsorption/reaction active sites.

Liu et al. found that a high density of surface defects can be maintained in Co_3O_4 catalysts obtained via mechanical milling of citric acid and cobalt basic carbonate [22]. The catalysts exhibited superior activity for propane total oxidation ($T_{100} = 240$ °C), in which the high concentration of superficial electrophilic oxygen (O^-) species played a key role. Tang et al. tuned the surface properties of Co_3O_4 nanoparticles with a diluted acid treatment strategy [16]. The acid leached-Co_3O_4

Fig. 3. Schematic diagram of facet-dependent Mn doping on Co_3O_4 crystals with {100} and {111} facets for catalytic oxidation of CO, propene, and propane [42].

nanoparticles possessed more surface defects and chemisorbed oxygen species than the pristine, which greatly boosted their propane oxidation activity. Moreover, the modified-Co_3O_4 showed much better performance and stability than the commercial 1%Pt (or Pd)/Al_2O_3 and self-made 1%Pt (or Pd)/CeO_2.

Yao et al. synthesized La-doped Co_3O_4 catalysts with various La/(La+Co) atomic ratios by a hydrothermal route [46]. They found that La doping resulted in a highly defective Co_3O_4 structure with abundant oxygen vacancies, favoring the activation and adsorption of gaseous propane and oxygen. Among the studied catalysts, La-Co_3O_4 with La/(La+Co) molar ratio of 1.8% showed the best propane combustion performance ($T_{90} = 264$ °C). As shown in Fig. 4, Zhu et al. developed an alkaline-earth metal (Mg and Ca) doping-etching strategy to regulate surface defects and lattice oxygen species in Co_3O_4 catalyst [57]. Co_3O_4 catalysts obtained by this strategy exhibited increased specific surface area, better low-temperature reducibility, and enhanced oxygen mobility. 5%Ca doped-etched Co_3O_4 catalyst showed the best propane oxidation performance ($T_{90} = 260$ °C), as well as decent long-term durability and reusability in the presence of 2.5 vol% water. Sun et al. showed that 3% of Cu doping in Co_3O_4 nanorods could activate the Co−O bond by enhancing the electrophilicity of adjacent O and creating defective structures, resulting in abundant surface-active oxygen species and facile activation of C−H bond in propane total oxidation [63]. Our group investigated the effect of different metals (Mn, Cu, Ni, and Fe) doping on the physicochemical properties and redox ability of Co_3O_4 [31]. The propane oxidation activity follows the order of Mn-Co_3O_4 > Fe-Co_3O_4 ≈ Mn-Co_3O_4 > Cu-Co_3O_4. Mn-doped Co_3O_4 exhibited the highest catalytic activity in propane oxidation in both dry and humid conditions, while Fe doping was beneficial in enhancing the water resistance of Co_3O_4. By a simple citrate sol-gel method, we obtained low-content Zr-doped Co_3O_4 catalysts and applied them in the catalytic oxidation of propane [50]. Doping 1% Zr into Co_3O_4 significantly improved the catalytic performance ($T_{90} = 241$ °C), which was mainly associated with the increase in surface defects and active oxygen species. Similarly, we investigated the effect of Y content on propane total oxidation over the Y-modified Co_3O_4 [54]. We found that Y addition inhibited the growth of Co_3O_4 crystalline and produced high-surface-area Co_3O_4 catalysts. Proper Y incorporation greatly promoted the reducibility and increased the number of surface oxygen species of the Y-Co_3O_4 catalysts, whereas excess Y accumulated on the surface to form yttrium carbonate species, covering the catalytic sites. The optimal atomic ratio of Y/(Co+Y) was 1%. Y acted as a promoter to modify the textural and redox properties of Co_3O_4 while Co_3O_4 coupled with abundant oxygen vacancies play the role of oxidizing propane.

4. Composite Co_3O_4 for propane total oxidation

Although single Co_3O_4 catalysts are active for propane oxidation, it is attractive to introduce a second component, which may bring the benefits of better adsorption/desorption ability, newly formed active interface, synergistic redox capacity, and higher concentration of surface species, etc. Among the composite Co_3O_4 catalysts, Ce-Co, Ni-Co, and Mn-Co systems are the most studied and demonstrate excellent propane oxidation performance.

Luo et al. constructed a set of mesoporous Co_3O_4-CeO_2 catalysts (S_{BET} > 100 m^2 g^{-1}) by a CTAB-templated method and applied them in propane oxidation [11]. The best activity was obtained when the Co/(Co + Ce) atomic ratio is 30%, due to the presence of the largest amounts of surface lattice oxygen species in Co_3O_4 crystallites. Li et al. prepared micro/mesoporous composite $CoCeO_x$ catalysts by a bi-template (P123 and SDS) sol-gel method [17]. The catalyst with a Co/Ce molar ratio of 1 exhibited the best propane oxidation performance ($T_{50} = 217$ °C), which could be ascribed to its high surface area ($S_{BET} = 131$ m^2 g^{-1}), excellent reducibility, and a large number of active oxygen species. Similarly, Zhang et al. obtained Co-Ce spinel oxides by a citrate complexing method and evaluated their catalytic performance in propane total
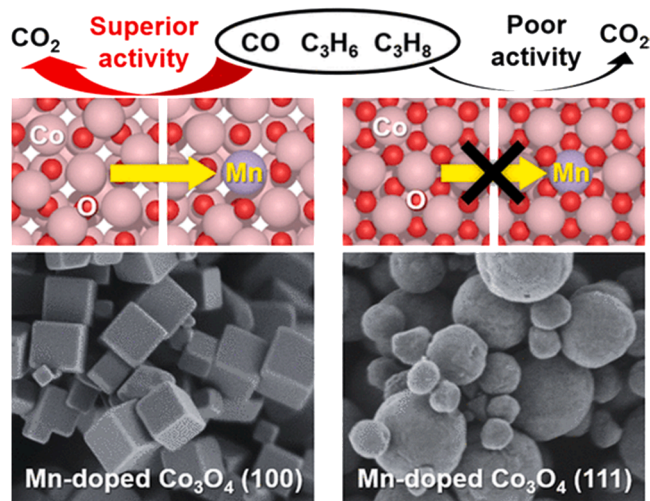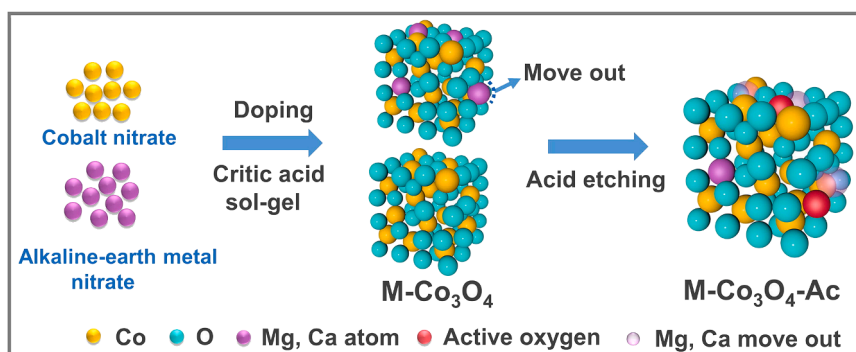
Fig. 4. Schematic diagram of defect engineering synthesis of Co_3O_4 by an alkaline-earth metal doping-etching strategy [57].

oxidation [18]. Catalyst $Co_2Ce_1O_x$ converted 50% of propane at 220 °C, which is much lower than single Co_3O_4. The incorporation of Ce into the Co_3O_4 spinel caused lattice distortion, weakened the Co−O bond, and improved the reducibility of Co^{3+}, which played a key role in propane total oxidation. Zhu et al. prepared Co_3O_4-CeO_2 composites with various Co/Co + Ce) molar ratios by a citrate sol-gel method and examined their propane total oxidation performance [35]. Among these catalysts, $CoCeO_x$ with a Co/Co + Ce) molar ratio of 70% exhibited the optimal performance (T_{90} = 310 °C), owing to the strong Co_3O_4-CeO_2 interaction that greatly enhanced the redox ability of the catalysts. By a mul-tifluidic coaxial electrospinning method, Feng et al. manufactured a core-shell CeO_2 @Co_3O_4 nanofiber catalyst for propane total oxidation [39]. The Co_3O_4 shell with small size and good reducibility reacted readily with propane while the CeO_2 core with abundant oxygen vacancies could promote the oxidation rate. Moreover, the continuous grain boundary in CeO_2 @Co_3O_4 favored the fast transfer of lattice oxygen species, which served as the dominant active oxygen species participating in propane oxidation. CeO_2 @Co_3O_4 showed better propane oxidation activity than CeO_2/Co_3O_4 due to a larger amount of lattice oxygen species and faster propane absorption capacity. It is well-known CeO_2 possesses excellent thermal stability. Introducing CeO_2 into Co_3O_4 catalysts could probably enhance their sintering resistance, which receive little attention and should worth exploring.

Ren et al. found that the incorporation of Ni into the Co_3O_4 spinel lattice could not only enhance the surface lattice oxygen mobility but also promote the desorption of CO_2 from the surface by forming unstable carbonates in propane oxidation [65]. The propane oxidation activity of Ni-Co_3O_4 increased while the structural stability decreased with Ni content. Therefore, a balance between activity and stability should be considered. Cai et al. synthesized a series of NiO-Co(x) with various Co/(Co+Ni) molar ratios (x = 0.05 −0.4) via a facile co-precipitation method and used them for propane combustion [15]. A highly dispersed Co_3O_4 nanocrystalline on Ni–Co–O solid solution was obtained when x = 0.3, which showed a higher propane oxidation rate than pure Co_3O_4 and NiO, due to the synergistic effects between Co_3O_4 and Ni–Co–O solid solution with high oxygen mobility. Zhang et al. built a spinel $NiCo_2O_4$ catalytic system with multi-defects by Na-assisted milling of hydrothermally prepared $NiCo_2O_4$ [59]. They proposed that Ni incorporation into Co_3O_4 spinel produced cationic defects, Na etching generated anionic defects, and mechano-milling exposed surface defects. The Na-etched $NiCo_2O_4$ exhibited a larger specific surface area, more oxygen vacancies, and enhanced oxygen mobility than Na-etched Co_3O_4, pristine $NiCo_2O_4$, and original Co_3O_4. As a result, it showed impressive propane oxidation performance (T_{90} = 194 °C). Although this Na assisted milling strategy can bring abundant anionic defects for $NiCo_2O_4$ spinel, it requires costly operating condition of an Ar protected glove box, which restrict its practical applications.

Faure et al. fabricated $Co_xMn_{3-x}O_4$ (0 ≤ x ≤ 3) oxides via mild decomposition of $Co_{x/3}Mn_{(3-x)/3}C_2O_4 \bullet 2H_2O$ at ca. 200 °C and followed calcination at 300 °C [12]. Co-Mn oxides with cubic spinel structure and

particularly high surface areas ($S_{BET} > 220$ m^2 g^{-1}) were obtained when x = 0.9 − 2.3. Catalyst $Co_{2.3}Mn_{0.7}O_4$ exhibited the best propane oxida-tion activity due to both a large surface area and a high cobalt content. Wu et al. used a facile inverse coprecipitation strategy to prepare Co−Mn oxide catalysts with different Co/Mn molar ratios and applied them for propane total oxidation [29]. The $Co_2Mn_1O_\delta$ catalyst was characterized by a Co−Mn solid solution spinel structure, a porous core−shell morphology, rich surface active Co^{3+}, and absorbed oxygen species. Therefore, it exhibited not only the best propane oxidation ac-tivity among the studied catalysts but also excellent water resistance and CO_2 tolerance. By a simple self-redox route, Li et al. synthesized amor-phous Co-Mn composite oxides for propane low-temperature oxidation [41]. Compared with spinel $Co_1Mn_3O_x$ with low defect content, the amorphous $Co_1Mn_3O_x$ with highly defective structure, weak Mn−O bond strength, good low-temperature reducibility, and ample reactive surface lattice oxygen showed much better activity in propane miner-alization (T_{90} = 207 °C).

By a citrate sol-gel method, Liao et al. synthesized Co-Cr composite oxides with various Co/Cr molar ratios for propane total oxidation [36]. The best activity was achieved at a Co/Cr molar ratio of 1:2, which is jointly determined by the surface acidity that affects propane adsorption and low-temperature reducibility that affects oxygen activation (Fig. 5). He et al. developed a range of Co-Zr composite oxides for propane combustion using a citrate sol-gel method [56]. The Co-Zr catalyst with a Co/Zr molar ratio of 4 showed the best catalytic performance among
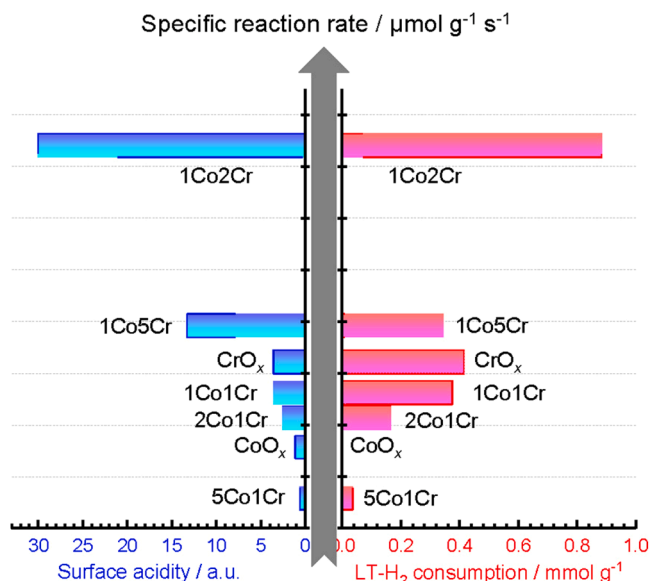

Fig. 5. Effects of the surface acidity and low-temperature reducibility on the propane oxidation rates of the catalysts [36].

the studied catalysts (T_{90} = 242 °C) as well as decent water resistance. The introduction of Zr produced more reactive Co^{3+} and oxygen species by forming Co-Zr solid solution, leading to significantly enhanced redox ability and surface oxygen mobility.

Yao et al. obtained Co_3O_4 nanoparticles well dispersed on the $LaCoO_3$ surface via acidic H_2O_2 treatment of $LaCoO_3$ [23]. The constructed Co_3O_4-$LaCoO_3$ composite exhibited much better performance towards propane combustion (T_{50} = 254 °C) compared with bare $LaCoO_3$ (T_{50} = 338 °C) due to the exposure of more Co sites and the increased concentration of oxygen vacancies. Wu et al. obtained Co-Al composite oxides from hydrothermally synthesized hydrotalcites and treated them with an ammonia atmosphere [61]. The results showed that ammonia treating produced a high quantity of oxygen vacancies by both the N doping effect and the reduction of Co^{3+} to Co^{2+}. The Co-Al oxide treated with NH_3 at 400 °C for 4 h exhibited the best propane oxidation performance (T_{90} = 266 °C). The in-situ DRIFT analysis revealed that the propylene and formate intermediates during the propane oxidation process decomposed easier over the N-doped Co-Al oxide compared with the pristine Co-Al oxide.

5. Supported Co_3O_4 for propane total oxidation

To enhance the thermal stability of the active phase and lower the cost for practical application, it is necessary to support Co_3O_4 on carriers. Solsona et al. prepared Co_3O_4/Al_2O_3 series via impregnation and investigated the effect of support nature (alpha, gamma, and mesoporous Al_2O_3) and Co loading (5, 20, 50 wt%) [10]. The catalytic activity is proportional to Co loading whereas inversely proportional to the specific surface area of Al_2O_3. This can be explained by the formation of active Co_3O_4 particles at high Co loading and inactive Co–O–Al species at high surface area support. To address this issue, Cai et al. developed a simple reduction-passivation strategy to adjust the Co–Al interaction in Co_3O_4/Al_2O_3 catalysts [28]. The reduction-passivation treatment weakened the Co–Al interaction and generated abundant active Co_3O_4 particles highly dispersed on the outer-layer of Al_2O_3 support, which greatly promoted the propane oxidation activity. A similar reduction-oxidation strategy was adopted by Liu et al. to tailor the Co_3O_4 size and state in Co_3O_4/ZSM-5 catalysts [51]. Oxidizing the pre-reduced 25%Co_3O_4/ZSM-5 catalyst in the propane-oxygen mixture atmosphere (2% O_2 + 0.2% C_3H_8 + N_2) decreased the Co_3O_4 size from 24.4 to 13.4 nm, increased the contents of reducible Co^{3+} and lattice oxygen species in the catalyst, which contributed greatly to the improved propane oxidation activity. Zhu et al. loaded Co_3O_4 onto ZSM-5 through impregnation (IM), deposition precipitation (DP), and hydrothermal (HT) methods and compared their activity with bulk Co_3O_4 and 1.5 wt% Pd/ZSM-5 for propane oxidation [44]. The Co_3O_4/ZSM-5 series showed superiority in propane oxidation activity to bulk Co_3O_4 and 1.5 wt% Pd/ZSM-5. Among the Co_3O_4/ZSM-5 series, the activity ranks as follows: HT > DP > IM. The reducibility and quantity of Co^{3+}, as well as the content and mobility of surface lattice oxygen, are reported to be the key factors of excellent catalytic activity. Aparicio et al. prepared Co_3O_4/SiO_2 catalysts with different Co loading (1, 5, 10, and 15 wt%) by impregnation [66]. Co_3O_4/SiO_2 with 5 wt% Co showed the best performance in propane oxidation due to the good dispersion of the Co_3O_4 phase. Zhang et al. fabricated nano-Co_3O_4 catalysts highly dispersed on SiO_2 via a surface-complexation route using Co(III) ammine hydroxo complexes [14]. The developed method could achieve desired cobalt loading, particle size control, and anti-sintering resistance. The obtained catalysts showed superior reducibility and propane oxidation activity to silica-supported CoO and Co-phyllosilicates. Todorova et al. prepared single and binary cobalt and manganese oxides supported on SBA-15 using a "two-solvent'' technique [21]. They found that for Co/SBA-15 catalysts, the Co_3O_4 nanoclusters were mainly on the surface and partially in the pore channel of SBA-15, while for Mn/SBA-15 catalysts, MnO_x species predominantly filled the SBA-15 channels and formed nanowires. In the case of CoMn/SBA-15, both

nanowires in the channels and small nanoparticles on the surface were observed. Among the studied catalysts, single Co/SBA-15 is the most active one for propane total oxidation owing to the presence of active Co^{3+} species on the surface. Using a hydrothermal-assisted precipitation-deposition method, Liu et al. supported 10 wt% Fe-Co, Ni-Co, and Cu-Co on CeO_2 nanorods with a Me/Co molar ratio of 1:2 [27]. The Me-Co oxides catalysts showed similar low-temperature propane oxidation performance, which was worse than single Co oxide catalyst, while the Ni-Co/CeO_2 catalyst exhibited much better performance than others at temperatures above 330 °C. Zha et al. decorated amorphous SiO_2 nanotubes with Co_3O_4 nanoparticles for propane total oxidation [40]. This catalyst can achieve 100% propane conversion at 240 °C, which was much lower than that of commercial SiO_2-supported Co_3O_4 (330 °C). Zha et al. supported the Co_3O_4 catalyst on the molten salt-treated halloysite by a wet impregnation method and then modified the catalyst by Fe_2O_3 using a urea deposition method [60]. The effect of Co loading and Fe content on the propane combustion performance of the catalyst were investigated. They found that 15 wt% Co loading was optimal for propane combustion, while 2 wt% Fe modification achieved the best promotional effect. Recently, we supported Co_3O_4 catalysts on a family of MWW zeolites (MCM-22, MCM-36, and MCM-56) by impregnation [48]. The effects of textural characteristics and Brønsted acid sites concentration of MWW zeolite support, as well as cobalt loading on propane oxidation activity were studied (Fig. 6). We found that high external surface and silanol groups of the support were against the reducibility of Co_3O_4. Cobalt−support interaction increased with enhancing Brønsted acid site amounts of the support, decreasing the low-temperature reducibility. MCM-22 demonstrated to be the optimal support for Co_3O_4 catalysts. The propane oxidation performance of Co_3O_4/MCM-22 catalysts increased with increasing Si/Al and cobalt content, consistent with the amount of low-temperature reducible Co_3O_4.

6. Mechanism of propane total oxidation over Co_3O_4-based catalysts

There have been three reaction mechanisms proposed for VOCs total oxidation over a catalyst (Fig. 7) [109]: i) Mars-van Krevelen (MVK) model, which involves two steps, first, the absorbed VOCs react with oxygen in the catalyst, then the resultant reduced sites are regenerated via the replenishment of gaseous oxygen or oxygen atoms in the bulk; ii) Langmuir-Hinshelwood (L-H) model, assuming that the reaction occurs between the adsorbed VOCs and the adsorbed oxygen species; iii) Eley-Rideal (E-R) model, similar to L-H model except that the reaction proceeds between the adsorbed oxygen species and the VOCs in the gas phase. Generally, the reaction mechanism is governed by both the type of VOCs and the properties of the catalyst. Regarding propane total oxidation over Co_3O_4-based catalysts, both MVK and L-H mechanisms were proposed by researchers based on different Co_3O_4 systems, where surface lattice oxygen species and surface adsorbed oxygen species played a key role, respectively.

Ma et al. probed the mechanism of propane total oxidation over Co_3O_4 nanorods using Pt/Al_2O_3 catalysts as a comparison [34]. As shown in Fig. 8, over both catalysts, extracting hydrogen from C−H bonds of propane was the kinetically relevant step, which turns propane into C_3H_7O* species. Then the C_3H_7O* species dissociated and were oxidized into carboxylates (formate, acetate, etc.). Finally, the carboxylate species were completely oxidized into CO_2 and H_2O. Propane oxidation over Co_3O_4 nanorods proceeded via the L-H mechanism, in which the rate-determining step was the activation of propane adsorbed on two adjacent oxygen atoms of Co_3O_4 by extracting hydrogen from the C–H bonds. On the other hand, propane oxidation over Pt/Al_2O_3 catalysts obeyed the E-R mechanism, in which the activation of gaseous propane on an adjacent oxygen atom and a vacant site was the rate-determining step.

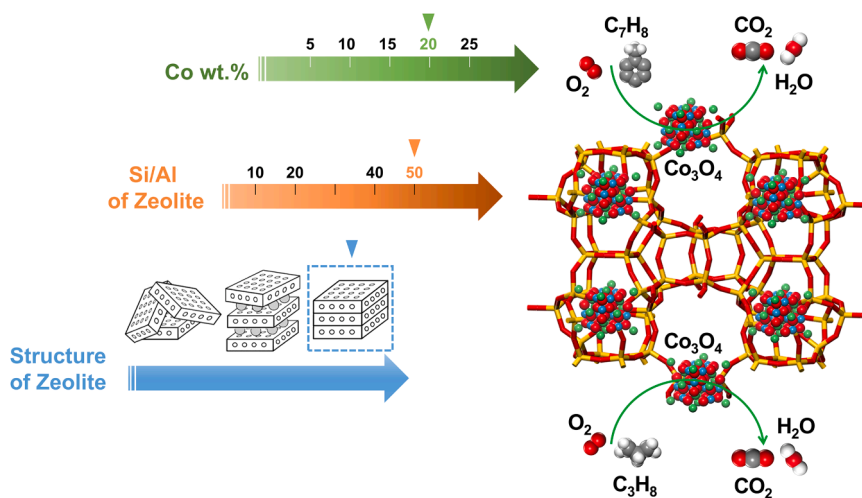Zhu et al. proposed a possible propane oxidation pathway over

Fig. 6. Schematic diagram of rational design of Co/MWW zeolite catalysts for VOCs oxidation [48].
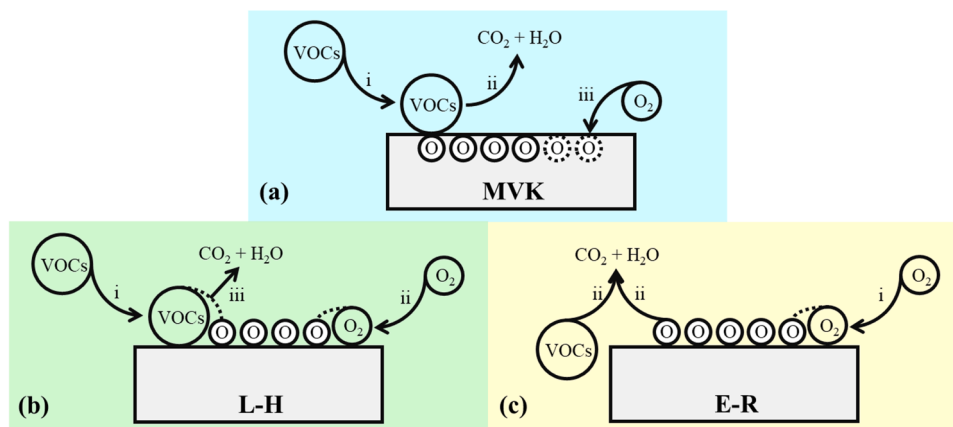

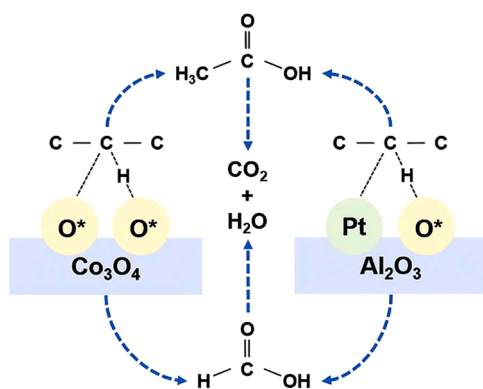**Fig. 7.** Schematic diagram of (a) MVK, (b) L-H, and (c) E-R model [109].

Fig. 8. Schematic diagram of propane oxidation mechanism over Co_3O_4 nanorods and Pt/Al_2O_3 catalysts [34].

Co_3O_4 catalysts (Fig. 9) [47,57]. Gaseous C_3H_8 was first chemically adsorbed on Co_3O_4 and then activated by surface-active oxygen. Next, the reaction between the activated C_3H_{8-n} species and the surface-active oxygen species broke the C−C bonds or other C−H bonds, producing carboxylate (formate/acetate) or carbonate intermediates. On the other hand, some surface-accumulated species like acetone and aliphatic ester group reacted with the surface-active oxygen species to form the carboxylate or carbonate intermediate. These carboxylate or carbonate

intermediates would be finally oxidized into CO_2 and H_2O. Simultaneously, gaseous oxygen adsorbed on the catalyst surface can be activated to replenish active oxygen species.

Over Co_3O_4 and $CoCeO_x$-70 catalysts, Zhu et al. proposed a possible MVK reaction mechanism of propane oxidation [35]. Propane is first adsorbed onto the superficial lattice oxygen, then the adsorbed propane is decomposed into carbonate species which are subsequently oxidized into acetone and aliphatic ester species. Thereafter, the ν(C═O) species are converted into CO_2 and H_2O. The consumed lattice oxygen is replenished by gaseous oxygen, completing a catalytic cycle. A similar MVK reaction mechanism was demonstrated by Feng et al. over CeO_2@Co_3O_4 and CeO_2/Co_3O_4 catalysts [39]. The detailed propane oxidation pathway was described as follows, $CH_3 −CH_2 −CH_3 \rightarrow CH_2 ═CH−CH_3$ $\rightarrow CH_2 ═CH−CHO \rightarrow CH_2 ═CH−COOH \rightarrow CO_2 + H_2O$. Wu et al. pointed out that propane total oxidation over Co-Al and N-doped Co-Al oxides was dominated by the L-H mechanism, in which surface-adsorbed oxygen species are more active than lattice oxygen species [61]. The detailed propane oxidation pathway can be described as follows: propane → propene → formate → CO_2. Li et al. investigated the propane degradation mechanism over amorphous $Co_1Mn_3O_x$ catalysts by in situ DRIFTS spectra [41]. They stressed the crucial role surface lattice oxygen played in propane total oxidation proceeded by the MVK mechanism. Propane was first adsorbed on the surface of the catalyst; then the C−H bond of propane was activated by the catalyst, achieving propane dehydrogenation; next, the C═C bond of propene was broken and oxidized into aldehydes, carboxylic acid, carbonate species; finally,
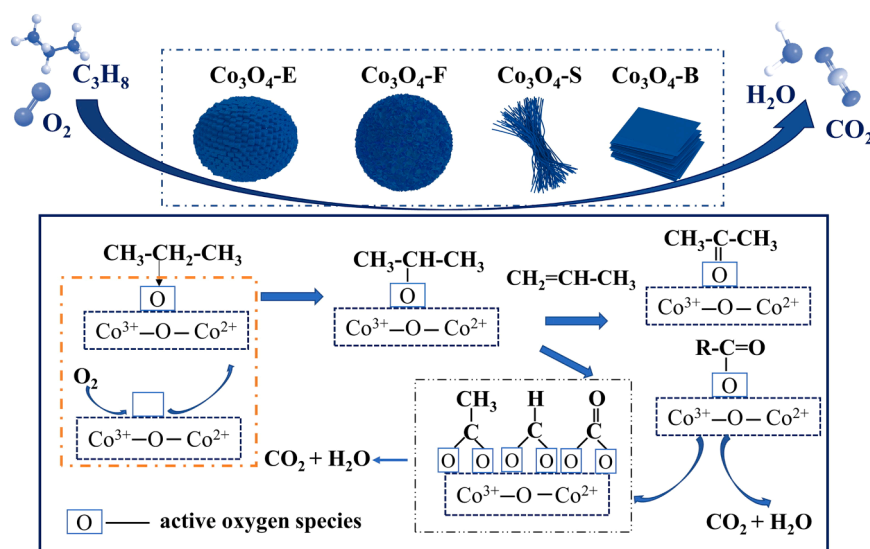
Fig. 9. Schematic diagram of propane oxidation mechanism over Co_3O_4 catalysts with various morphologies [47].

these intermediate species were completely oxidized into CO_2 and H_2O.

Zha et al. probed the propane oxidation pathways over the Co_3O_4 catalysts embedded in amorphous SiO_2 nanotubes (Co/SiO_2 −N) and Co_3O_4 catalysts supported on commercial SiO_2 (Co/SiO_2 −I) [40]. They proposed two possible reaction pathways, one is the carbonate species pathway following the MVK mechanism (Fig. 10a), in which propane was first oxidized by the surface lattice oxygen species (O_L). The other is the acrylate species pathway obeying the E − R mechanism (Fig. 10b), in which gaseous O_2 activated on the catalyst surface (O_S) reacted directly with gaseous propane. Propane total oxidation over Co/SiO_2 −N catalysts could proceed via both the carbonate and acrylate pathways, while only the carbonate species pathway took place over Co/SiO_2 −I catalysts. Liu et al. confirmed by in situ DRIFT the MVK mechanism for propane oxidation over the 25%Co_3O_4/ZSM-5 catalysts, in which the surface lattice O^{2-} species in Co_3O_4 was first reduced by propane and then replenished by gaseous O_2 [51]. Their kinetic study of propane oxidation over 25%Co_3O_4/ZSM-5 revealed a positive reaction order of propane and a negative reaction order of oxygen, indicating that the

increased oxygen partial pressure would inhibit the catalytic activity. They speculated that gaseous O_2 could compete with propane for the same adsorption sites, which was not conducive to propane activation.
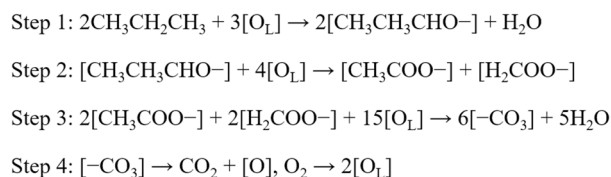
7. Poisoning effect on propane total oxidation over Co_3O_4-based catalysts

In practical applications, it is of great importance for a catalyst to maintain its activity in complex conditions. Generally, propane total oxidation over Co_3O_4 catalysts could be deactivated by the presence of H_2O, CO_2, or SO_2 in the reaction gas through competitive adsorption, chemical passivation, active site covering, or pore blocking. On the other hand, the residual alkali metal or chlorine in the Co_3O_4 catalysts can also affect their activity. We summarized in this section various poisoning effects on propane total oxidation over Co_3O_4-based catalysts.

7.1. Effect of H_2O or CO_2

As the product of propane mineralization, H_2O or CO_2 hardly affects the catalytic performance when it is present in the catalytic system with a low concentration. However, high humidity and/or high concentration of CO_2 often have a severe inhibitory effect on Co_3O_4-based catalysts for propane combustion. H_2O or CO_2 molecules can compete with propane or oxygen for the adsorption sites. Moreover, hydroxyl groups can be formed by the adsorption of H_2O molecules on the Co_3O_4 surface while carbonate species can accumulate via the adsorption of CO_2 molecules on the Co_3O_4 surface, both of which may occupy the vacancies for oxygen activation, thus degrading catalytic activity. Li investigated the inhibitory effect of 3.1 vol% H_2O on propane oxidation over various Co_3O_4 catalysts and revealed that H_2O would chemisorb in oxygen vacancy and inhibit both the adsorption of propane and the mobility of surface lattice oxygen [62]. Zhu et al. found that 2.5 vol% H_2O in the reaction gas can suppress the adsorption and activation of propane on the Co_3O_4 surface and thus significantly reduce the propane oxidation efficiency [47]. A similar negative effect was observed when they introduced H_2O or CO_2 in propane oxidation over a Co-Ce oxide catalyst [35]. The inhibitory effect of H_2O was more serious than that of CO_2 on the Co-Ce oxide catalyst. We have examined the effects of both H_2O and CO_2 on propane oxidation over a typical Co_3O_4 catalyst [30]. The T_{50} value rase from 199 °C to 218 °C and 207 °C, respectively when H_2O or CO_2 was introduced, suggesting that Co_3O_4 is more sensitive to H_2O poisoning than CO_2 poisoning. By cutting off H_2O or CO_2 stream, the propane conversion was restored, indicating the reversibility of this

(a) Carbonate species pathway

Step 1: $2CH_3CH_2CH_3 + 3[O_L] \rightarrow 2[CH_3CH_3CHO-] + H_2O$

Step 2: $[CH_3CH_3CHO-] + 4[O_L] \rightarrow [CH_3COO-] + [H_2COO-]$

Step 3: $2[CH_3COO-] + 2[H_2COO-] + 15[O_L] \rightarrow 6[-CO_3] + 5H_2O$

Step 4: $[-CO_3] \rightarrow CO_2 + [O], O_2 \rightarrow 2[O_L]$

(b) Acrylate species pathway

Step 1: $O_2 \rightarrow 2[O_S]$

Step 2: $2CH_3CH_2CH_3 + 3[O_S] \rightarrow 2[CH_3CH_3CHO-] + H_2O$

Step 3: $[CH_3CH_2CH_2O-] + 2[O_S] \rightarrow [CH_2CHCOO-] + 2H_2O$

Step 4: $2[CH_2CHCOO-] + 3[O_S] \rightarrow 2[CH_2COCOO-] + H_2O$

Step 5: $[CH_2COCOO-] + 4[O_S] \rightarrow 3CO_2 + H_2O$
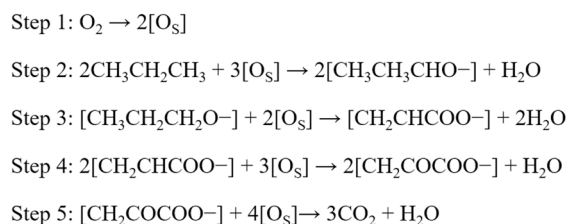
Fig. 10. Schematic diagram of two propane oxidation pathways over supported Co_3O_4 catalysts (a) carbonate species pathway, (b) acrylate species pathway [40].

deactivation. In addition, increasing H_2O content from 0 to 4.4 vol% led to a gradual decrease of the propane oxidation performance over Co_3O_4 while further increasing H_2O content to 8.8 vol% partially recovered the catalytic performance. We also investigated the effects of H_2O, CO_2, and NO introduction in the long-term propane oxidation test over single Co_3O_4 and Cu-Co mixed oxide [53]. The results showed that H_2O and NO led to a larger propane conversion drop than CO_2. The propane oxidation inhibition effect caused by H_2O or CO_2 could be perfectly eliminated after removing H_2O or CO_2 from the inlet gas, whereas the severe deactivation caused by NO introduction was only partially reversible. Li et al. studied the role of H_2O in propane total oxidation over Co_3O_4 catalysts with different morphology [62]. They found that H_2O could compete with propane for the adsorption sites and the chemically adsorbed H_2O would hinder the mobility of lattice oxygen in Co_3O_4, thereby inhibiting the propane oxidation activity. Interestingly, the inhibition effect of H_2O on Co_3O_4 nanorods mainly exposing {111} facets is minimal thanks to the low propane competitive adsorption energy and H_2O adsorption energy of the Co_3O_4 {111} facets.

7.2. Effect of SO_2

SO_2 is well-known to poison the Co_3O_4 surface and decrease the catalytic activity of Co_3O_4. Specifically, SO_2 can be adsorbed on the Co_3O_4 surface, compete with the active site of VOCs oxidation, and react with Co_3O_4 to form inactive cobalt sulfate species. Zha et al. reported that propane total oxidation over Co_3O_4/halloysite catalysts can be irreversibly inhibited by the presence of SO_2 [60]. They attributed this poisoning effect to the formation of thermally stable cobalt sulfate species, which decreased the number of cobalt active sites. To enhance the SO_2 tolerance of the catalyst, they introduced Fe_2O_3 as a catalytic promoter. The results showed that Fe_2O_3 in the Fe_2O_3-Co_3O_4/halloysite catalyst can protect the cobalt active components by the formation of thermally unstable iron sulfate species with SO_2 (Fig. 11). As a result, the activity deactivation caused by SO_2 was alleviated. Tang et al. showed that the full conversion of propane over the Co_3O_4 catalyst derived from chemical leaching could be maintained in the presence of 5 ppm of SO_2 for 6 h at 280 °C [16]. Liu et al. reported a small inhibitory effect of SO_2 on mesoporous Co_3O_4-supported Au catalysts for toluene oxidation [110]. SO_2 cannot be adsorbed on the highly dispersed Au but on the

Co_3O_4 surface to form some cobalt sulfates, causing slightly degraded activity. Bao et al. studied the effect of SO_2 concentration on porous $Co_xMn_{1-x}O_y$ catalysts for propene total oxidation [73]. They found that 20 and 100 ppm of SO_2 caused a negligible decrease in propene oxidation performance while 500 ppm of SO_2 had an obvious inhibition effect. The results demonstrated the competitive SO_2 resistance of $Co_xMn_{1-x}O_y$ catalysts.

7.3. Effect of alkali metal

Although alkali metals have a promotional effect on Co_3O_4 catalysts for HCHO and soot combustion [111,112], they appear to be a poison for propane total oxidation. Tang et al. deposited Na, K, and Li onto Co_3O_4 via impregnation to study their effects on propane total oxidation [19]. The results showed that alkali metals not only reduced the oxygen mobility of Co_3O_4 by inhibiting oxygen desorption at low temperature, but also strengthened CO and CO_2 adsorption on the surface of Co_3O_4 and contributed to surface carbonate species accumulation even at high temperature, which resulted in poor propane oxidation performance. The more alkali metals introduced the more severe the poisoning effect. Likewise, the residual sodium in Co_3O_4 synthesized by the sodium carbonate precipitating route was found to cause serious deactivation of the catalyst in propane total oxidation, which could be alleviated by thorough washing with water or acid [26,43]. Zha et al. found that propane oxidation over Co_3O_4/SiO_2 catalysts prepared via impregnation can be poisoned by K through decreasing oxygen mobility and inhibiting CO_2 desorption [40]. They developed a new strategy to enhance the alkali metal resistance of Co_3O_4 by embedding the Co_3O_4 nanoparticles in amorphous SiO_2 nanotubes, which could provide confined effects for Co_3O_4 and shielding alkali metal poisoning by changing the propane oxidation pathway (Fig. 12).

7.4. Effect of chlorine

Most catalysts can be poisoned by chlorine species [2]. The detrimental effect of chlorine on noble metal catalysts has been widely studied while little attention was paid to the role of chlorine residue on Co_3O_4 catalysts. Ren et al. obtained two Co_3O_4 nanowires using cobalt nitrate and cobalt chloride as cobalt sources and compared their propane combustion performance [65]. Co_3O_4-Cl exhibited lower propane oxidation activity than Co_3O_4-NO_3, especially in the low-temperature range. The residual surface chlorine species can passivate the Co−O bonds and decrease the mobility of lattice oxygen, thus leading to inferior activity. Likewise, an inhibitory effect of chlorine was found on Co_3O_4 catalysts for CO oxidation, which can be eliminated by washing the Co_3O_4 catalysts thoroughly with water [113]. Zhong et al. prepared Co_3O_4 catalysts using cobalt nitrate, sulfate, acetate, and chloride salts. Among the four catalysts, Co_3O_4 derived from cobalt chloride showed the worst catalytic performance due to its inferior redox ability, which confirmed the poisoning effect of chloride on Co_3O_4 catalysts indirectly [81].

8. Conclusions and perspectives

8.1. Conclusions

Co_3O_4-based catalysts demonstrate good prospects in propane total oxidation due to their unique physicochemical properties. The propane oxidation performance of single, composite, and supported Co_3O_4 catalysts fabricated by versatile routes was reviewed. The boosted propane oxidation activity of Co_3O_4-based catalysts is mainly related to the increased number of surface reactive oxygen species, enhanced low-temperature reducibility, and enlarged surface area. Propane total oxidation over Co_3O_4-based catalysts generally proceeds via an MVK mechanism, with carboxylates and carbonate species as main intermediates. H_2O or CO_2 reversibly inhibits propane oxidation by
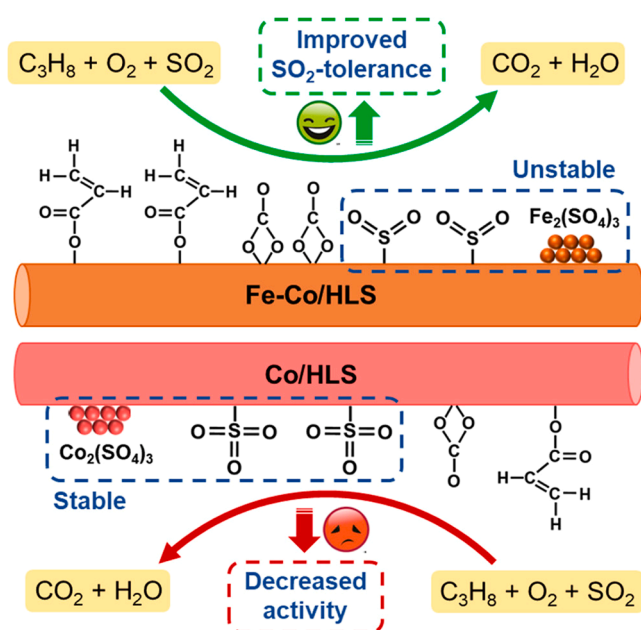

Fig. 11. Schematic diagram of propane total oxidation in the presence of SO_2 over Co/halloysite and Fe–Co/halloysite catalysts [60].
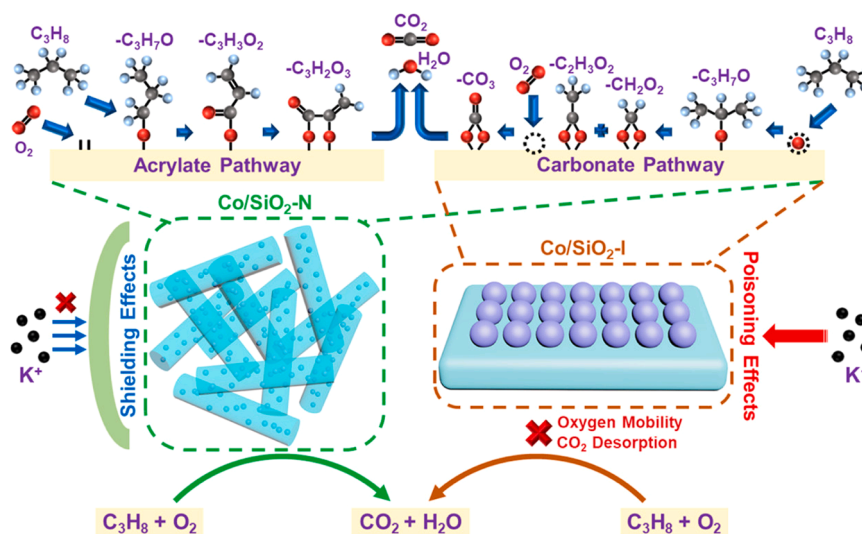
Fig. 12. Schematic diagram of propane total oxidation in the presence of alkali metals over Co/SiO$_2$–N and Co/SiO$_2$–I catalysts [40].

competitive adsorption with propane or oxygen molecules. Alkali metal or chlorine deactivates Co$_3$O$_4$ catalysts by passivating Co−O bonds and decreasing oxygen mobility. SO$_2$ poisons the active sites of Co$_3$O$_4$ by forming cobalt sulfate species.

8.2. Perspectives

Despite much work done and advances achieved, ongoing efforts are necessary to develop more efficient and robust Co$_3$O$_4$-based catalysts for practical industrial applications. The following aspects await further studies:

(1) Identification of the actual active sites in Co$_3$O$_4$-based catalysts for propane total oxidation. For instance, in a metal-doped Co$_3$O$_4$ system, it is sometimes confusing whether the oxygen vacancies created by metal doping or the metal dopant itself are the active sites, let alone the possible synergy between them. In some cases, the active sites for chemical adsorption of propane molecules and activation of oxygen molecules remain unclear. Therefore, systematic investigations are desired to clarify their respective contributions and roles in propane total oxidation.

(2) Precise control of defects in Co$_3$O$_4$ via green routes. Though various defect engineering methods have been developed to enhance the performance of Co$_3$O$_4$, current methods require complicated procedures or costly chemical treatment, which are environmentally unfriendly and unscalable. On the other hand, precise control of the type and concentration of defects in Co$_3$O$_4$ remains challenging, which makes it difficult to clarify the exact roles of anionic vs cationic defects and surface vs bulk defects of Co$_3$O$_4$ in propane total oxidation.

(3) Development of robust Co$_3$O$_4$-based catalysts via high entropy strategy. Co$_3$O$_4$ catalysts usually encounter sintering and poisoning issues in propane total oxidation. High entropy oxides have recently attracted much attention due to the advantages of high stability, abundant oxygen vacancies, and high dispersion of metal elements. Constructing high entropy Co$_3$O$_4$-based catalytic systems can bring multiple active sites and ultra-high stability, which may solve the problem of Co$_3$O$_4$ deactivation while improving the activity.

(4) Engineering of monoatomic or sub-nanoscale active CoO$_x$ catalysts. Currently, most studies focus on bulk Co$_3$O$_4$ or supported Co$_3$O$_4$ with high loading. With the soaring price of cobalt, it is desirable to disperse CoO$_x$ as single or sub-nanoscale clusters on

robust supports to expose more cobalt active sites and improve atom economy.

(5) Investigation of propane total oxidation over Co$_3$O$_4$-based catalysts in the presence of other VOCs or components (H$_2$O, CO$_2$, NO$_x$, SO$_2$). Industrial emissions are generally composed of multiple VOCs and impurities, inhibiting, independent or promoting effects can occur when propane is oxidized in mixtures. A comprehensive analysis of propane oxidation behavior in mixtures over Co$_3$O$_4$-based catalysts is crucial to the practical application. Revealing propane oxidation/deactivation mechanism in simulated realistic exhaust conditions can provide guidance for the design of Co$_3$O$_4$-based catalysts resistant to poisoning to meet the industrial demand.

Declaration of Competing Interest

The authors declare that they have no known competing financial interests or personal relationships that could have appeared to influence the work reported in this paper.

Data Availability

No data was used for the research described in the article.

Acknowledgement

References

[1] Y. Guo, M. Wen, G. Li, T. An, Recent advances in VOC elimination by catalytic oxidation technology onto various nanoparticles catalysts: a critical review, Appl. Catal. B Environ. 281 (2021), 119447, https://doi.org/10.1016/j.apcatb.2020.119447.

[2] C. He, J. Cheng, X. Zhang, M. Douthwaite, S. Pattisson, Z. Hao, Recent advances in the catalytic oxidation of volatile organic compounds: a review based on pollutant sorts and sources, Chem. Rev. 119 (2019) 4471–4568, https://doi.org/10.1021/acs.chemrev.8b00408.

[3] M.S. Kamal, S.A. Razzak, M.M. Hossain, Catalytic oxidation of volatile organic compounds (VOCs) – a review, Atmos. Environ. 140 (2016) 117–134, https://doi.org/10.1016/j.atmosenv.2016.05.031.

[4] J. González-Prior, R. López-Fonseca, J.I.I. Gutiérrez-Ortiz, B. de Rivas, Catalytic removal of chlorinated compounds over ordered mesoporous cobalt oxides synthesised by hard-templating, Appl. Catal. B Environ. 222 (2018) 9–17, https://doi.org/10.1016/j.apcatb.2017.09.050.

[5] S. Ojala, S. Pitkäaho, T. Laitinen, N. Niskala Koivikko, R. Brahmi, J. Gaálová, L. Matejova, A. Kucherov, S. Päivärinta, C. Hirschmann, T. Nevanperä, M. Riihimäki, M. Pirilä, R.L. Keiski, Catalysis in VOC Abatement, Top. Catal. 54 (2011) 1224–1256, https://doi.org/10.1007/s11244-011-9747-1.

[6] L.F. Liotta, H. Wu, G. Pantaleo, A.M. Venezia, Co_3O_4 nanocrystals and Co_3O_4–MO_x binary oxides for CO, CH_4 and VOC oxidation at low temperatures: a review, Catal. Sci. Technol. 3 (2013) 3085, https://doi.org/10.1039/c3cy00193h.

[7] Y. Lou, X.M. Cao, J. Lan, L. Wang, Q. Dai, Y. Guo, J. Ma, Z. Zhao, Y. Guo, P. Hu, G. Lu, Ultralow-temperature CO oxidation on an In_2O_3–Co_3O_4 catalyst: A strategy to tune CO adsorption strength and oxygen activation simultaneously, Chem. Commun. 50 (2014) 6835–6838, https://doi.org/10.1039/c4cc00036f.

[8] L. Wang, W. Hu, Z. Shang, X. Cao, Y. Guo, J. Li, Q. Gu, K. Li, X. Li, Regulating potassium state to enable the high performance of Co_3O_4 for catalytic oxidation, Fuel 335 (2023), 126968, https://doi.org/10.1016/j.fuel.2022.126968.

[9] R. Sanchis, A. García, F. Ivars-Barceló, S.H. Taylor, T. García, A. Dejoz, M. I. Vázquez, B. Solsona, Highly active Co_3O_4-based catalysts for total oxidation of light C1–C3 alkanes prepared by a simple soft chemistry method: effect of the heat-treatment temperature and mixture of alkanes, Materials 14 (2021) 7120, https://doi.org/10.3390/ma14237120.

[10] B. Solsona, T.E. Davies, T. Garcia, I. Vázquez, A. Dejoz, S.H. Taylor, Total oxidation of propane using nanocrystalline cobalt oxide and supported cobalt oxide catalysts, Appl. Catal. B Environ. 84 (2008) 176–184, https://doi.org/10.1016/j.apcatb.2008.03.021.

[11] J.-Y. Luo, M. Meng, Y.-Q. Zha, L.-H. Guo, Identification of the Active Sites for CO and C_3H_8 Total Oxidation over Nanostructured CuO−CeO_2 and Co_3O_4−CeO_2, Catal., J. Phys. Chem. C. 112 (2008) 8694–8701, https://doi.org/10.1021/jp800651k.

[12] B. Faure, P. Alphonse, Co–Mn-oxide spinel catalysts for CO and propane oxidation at mild temperature, Appl. Catal. B Environ. 180 (2016) 715–725, https://doi.org/10.1016/j.apcatb.2015.07.019.

[13] W. Zhang, F. Wu, J. Li, Z. You, Dispersion–precipitation synthesis of highly active nanosized Co_3O_4 for catalytic oxidation of carbon monoxide and propane, Appl. Surf. Sci. 411 (2017) 136–143, https://doi.org/10.1016/j.apsusc.2017.03.162.

[14] W. Zhang, F. Pan, J. Li, Z. Wang, W. Qin, J. Yin, F. Wu, Surface-complexation synthesis of silica-supported high-loading well-dispersed reducible nano-Co_3O_4 catalysts using Co^{III} ammine hydroxo complexes, Appl. Surf. Sci. 442 (2018) 83–91, https://doi.org/10.1016/j.apsusc.2018.02.094.

[15] T. Cai, J. Yuan, L. Zhang, L. Yang, Q. Tong, M. Ge, B. Xiao, X. Zhang, K. Zhao, D. He, Ni-Co-O solid solution dispersed nanocrystalline Co_3O_4 as a highly active catalyst for low-temperature propane combustion, Catal. Sci. Technol. 8 (2018) 5416–5427, https://doi.org/10.1039/c8cy01062e.

[16] W. Tang, W. Xiao, S. Wang, Z. Ren, J. Ding, P.-X. Gao, Boosting catalytic propane oxidation over PGM-free Co_3O_4 nanocrystal aggregates through chemical leaching: A comparative study with Pt and Pd based catalysts, Appl. Catal. B Environ. 226 (2018) 585–595, https://doi.org/10.1016/j.apcatb.2017.12.075.

[17] X. Li, X. Li, X. Zeng, T. Zhu, Correlation between the physicochemical properties and catalytic performances of micro/mesoporous $CoCeO_x$ mixed oxides for propane combustion, Appl. Catal. A Gen. 572 (2019) 61–70, https://doi.org/10.1016/j.apcata.2018.12.026.

[18] S. Zhang, S. Liu, X. Zhu, Y. Yang, W. Hu, H. Zhao, R. Qu, C. Zheng, X. Gao, Low temperature catalytic oxidation of propane over cobalt-cerium spinel oxides catalysts, Appl. Surf. Sci. 479 (2019) 1132–1140, https://doi.org/10.1016/j.apsusc.2019.02.118.

[19] W. Tang, J. Weng, X. Lu, L. Wen, A. Suburamanian, C.-Y.Y. Nam, P.-X.X. Gao, Alkali-metal poisoning effect of total CO and propane oxidation over Co_3O_4 nanocatalysts, Appl. Catal. B Environ. 256 (2019), 117859, https://doi.org/10.1016/j.apcatb.2019.117859.

[20] J. Yao, H. Shi, D. Sun, H. Lu, B. Hou, L. Jia, Y. Xiao, D. Li, Facet-dependent activity of Co_3O_4 catalyst for C_3H_8 combustion, ChemCatChem 11 (2019) 5570–5579, https://doi.org/10.1002/cctc.201901382.

[21] S. Todorova, J.L.L. Blin, A. Naydenov, B. Lebeau, H. Kolev, P. Gaudin, A. Dotzeva, R. Velinova, D. Filkova, I. Ivanova, L. Vidal, L. Michelin, L. Josien, K. Tenchev, Co_3O_4-MnO_x oxides supported on SBA-15 for CO and VOCs oxidation, Catal. Today 357 (2020) 602–612, https://doi.org/10.1016/j.cattod.2019.05.018.

[22] Q. Liu, L.-C.C. Wang, M. Chen, Y. Cao, H.-Y.Y. He, K.-N.N. Fan, Dry citrate-precursor synthesized nanocrystalline cobalt oxide as highly active catalyst for total oxidation of propane, J. Catal. 263 (2009) 104–113, https://doi.org/10.1016/j.jcat.2009.01.018.

[23] J. Yao, H. Lu, B. Hou, L. Jia, Y. Xiao, D. Li, Acidic H_2O_2 treatment of $LaCoO_3$ towards highly dispersed Co_3O_4 nanoparticles with excellent catalytic performance for C_3H_8 combustion, Catal. Commun. 135 (2020), 105830, https://doi.org/10.1016/j.catcom.2019.105830.

[24] K. Chen, W. Li, Z. Zhou, Q. Huang, Y. Liu, Q. Duan, Hydroxyl groups attached to Co^{2+} on the surface of Co_3O_4: a promising structure for propane catalytic oxidation, Catal. Sci. Technol. 10 (2020) 2573–2582, https://doi.org/10.1039/D0CY00265H.

[25] I. Driouch, W. Zhang, M. Heitz, J.L. Valverde, A. Giroir-Fendler, Total oxidation of toluene and propane over Co_3O_4 catalysts: Influence of precipitating pH and washing, Catalysts 10 (2020) 900, https://doi.org/10.3390/catal10080900.

[26] G. Chai, W. Zhang, Y. Guo, J.L. Valverde, A. Giroir-Fendler, The influence of residual sodium on the catalytic oxidation of propane and toluene over Co_3O_4 catalysts, Catalysts 10 (2020) 867, https://doi.org/10.3390/catal10080867.

[27] Z. Liu, J. Li, R. Wang, CeO_2 nanorods supported M−Co bimetallic oxides (M = Fe, Ni, Cu) for catalytic CO and C_3H_8 oxidation, J. Colloid Interface Sci. 560 (2020) 91–102, https://doi.org/10.1016/j.jcis.2019.10.046.

[28] T. Cai, W. Deng, P. Xu, J. Yuan, Z. Liu, K. Zhao, Q. Tong, D. He, Great activity enhancement of Co_3O_4/γ-Al_2O_3 catalyst for propane combustion by structural modulation, Chem. Eng. J. 395 (2020), 125071, https://doi.org/10.1016/j.cej.2020.125071.

[29] E. Wu, X. Feng, Y. Zheng, D. Lin, Y. Luo, Y. You, B. Huang, Q. Qian, Q. Chen, Inverse coprecipitation directed porous core–shell Mn–Co–O catalyst for efficient low temperature propane oxidation, ACS Sustain. Chem. Eng. 8 (2020) 5787–5798, https://doi.org/10.1021/acssuschemeng.0c01497.

[30] W. Zhang, J. Díez-Ramírez, P. Anguita, C. Descorme, J.L. Valverde, A. Giroir-Fendler, Nanocrystalline Co_3O_4 catalysts for toluene and propane oxidation: Effect of the precipitation agent, Appl. Catal. B Environ. 273 (2020), 118894, https://doi.org/10.1016/j.apcatb.2020.118894.

[31] W. Zhang, P. Anguita, J. Díez-Ramírez, C. Descorme, J.L. Valverde, A. Giroir-Fendler, Comparison of different metal doping effects on Co_3O_4 catalysts for the total oxidation of toluene and propane, Catalysts 10 (2020) 865, https://doi.org/10.3390/catal10080865.

[32] Z. Liu, L. Cheng, J. Zeng, X. Hu, S. Zhangxue, S. Yuan, Q. Bo, B. Zhang, Y. Jiang, Synthesis, characterization and catalytic performance of nanocrystalline Co_3O_4 towards propane combustion: Effects of small molecular carboxylic acids, J. Solid State Chem. 292 (2020), 121712, https://doi.org/10.1016/j.jssc.2020.121712.

[33] T. Garcia, S. Agouram, J.F. Sánchez-Royo, R. Murillo, A.M. Mastral, A. Aranda, I. Vázquez, A. Dejoz, B. Solsona, Deep oxidation of volatile organic compounds using ordered cobalt oxides prepared by a nanocasting route, Appl. Catal. A Gen. 386 (2010) 16–27, https://doi.org/10.1016/j.apcata.2010.07.018.

[34] L. Ma, Y. Geng, X. Chen, N. Yan, J. Li, J.W. Schwank, Reaction mechanism of propane oxidation over Co_3O_4 nanorods as rivals of platinum catalysts, Chem. Eng. J. 402 (2020), 125911, https://doi.org/10.1016/j.cej.2020.125911.

[35] W. Zhu, X. Chen, J. Jin, X. Di, C. Liang, Z. Liu, Insight into catalytic properties of Co_3O_4-CeO_2 binary oxides for propane total oxidation, Chin. J. Catal. 41 (2020) 679–690, https://doi.org/10.1016/S1872-2067(19)63523-0.

[36] W.M. Liao, P.P. Zhao, B.H. Cen, A.P. Jia, J.Q. Lu, M.F. Luo, Co–Cr–O mixed oxides for low–temperature total oxidation of propane: Structural effects, kinetics, and spectroscopic investigation, Chin. J. Catal. 41 (2020) 442–453, https://doi.org/10.1016/S1872-2067(19)63480-7.

[37] D. Lin, Y. Zheng, X. Feng, Y. You, E. Wu, Y. Luo, Q. Qian, Q. Chen, Highly stable Co_3O_4 nanoparticles-assembled microrods derived from MOF for efficient total propane oxidation, J. Mater. Sci. 55 (2020) 5190–5202, https://doi.org/10.1007/s10853-020-04368-1.

[38] Z. Liu, L. Cheng, S. Zhangxue, M. Huang, J. Zeng, S. Yuan, Q. Bo, B. Zhang, Y. Jiang, Enhancement of propane combustion activity over CoO_x catalysts by introducing C2–C5 diols, N. J. Chem. 45 (2021) 8795–8805, https://doi.org/10.1039/D1NJ00052G.

[39] X. Feng, F. Luo, Y. Chen, D. Lin, Y. Luo, L. Xiao, X. Liu, X. Sun, Q. Qian, Q. Chen, Boosting total oxidation of propane over $CeO_2@Co_3O_4$ nanofiber catalysts prepared by multifluidic coaxial electrospinning with continuous grain boundary and fast lattice oxygen mobility, J. Hazard. Mater. 406 (2021) 124695, https://doi.org/10.1016/j.jhazmat.2020.124695.

[40] K. Zha, H. Liu, L. Xue, Z. Huang, H. Xu, W. Shen, Co_3O_4 nanoparticle-decorated SiO_2 nanotube catalysts for propane oxidation, ACS Appl. Nano Mater. 4 (2021) 8937–8949, https://doi.org/10.1021/acsanm.1c01558.

[41] G. Li, N. Li, Y. Sun, Y. Qu, Z. Jiang, Z. Zhao, Z. Zhang, J. Cheng, Z. Hao, Efficient defect engineering in Co-Mn binary oxides for low-temperature propane oxidation, Appl. Catal. B Environ. 282 (2021), 119512, https://doi.org/10.1016/j.apcatb.2020.119512.

[42] J. Bae, J. Shin, H. Jeong, C. Choe, Y. Choi, J.W. Han, H. Lee, Facet-dependent Mn doping on shaped Co_3O_4 crystals for catalytic oxidation, ACS Catal. 11 (2021) 11066–11074, https://doi.org/10.1021/acscatal.1c01666.

[43] W. Zhang, K. Lassen, C. Descorme, J.L. Valverde, A. Giroir-Fendler, Effect of the precipitation pH on the characteristics and performance of Co_3O_4 catalysts in the total oxidation of toluene and propane, Appl. Catal. B Environ. 282 (2021), 119566, https://doi.org/10.1016/j.apcatb.2020.119566.

[44] Z. Zhu, G. Lu, Z. Zhang, Y. Guo, Y. Guo, Y. Wang, Highly active and stable Co_3O_4/ZSM-5 catalyst for propane oxidation: effect of the preparation method, ACS Catal. 3 (2013) 1154–1164, https://doi.org/10.1021/cs400068v.

[45] Y. Jian, M. Tian, C. He, J. Xiong, Z. Jiang, H. Jin, L. Zheng, R. Albilali, J.-W. W. Shi, Efficient propane low-temperature destruction by Co_3O_4 crystal facets engineering: Unveiling the decisive role of lattice and oxygen defects and surface acid-base pairs, Appl. Catal. B Environ. 283 (2021) 119657, https://doi.org/10.1016/j.apcatb.2020.119657.

[46] J. Yao, H. Lu, B. Hou, Y. Xiao, L. Jia, D. Li, J. Wang, The promotional effect of La dopant on Co_3O_4 catalytic performance towards C_3H_8 combustion, Catal. Lett. 151 (2021) 1745–1754, https://doi.org/10.1007/s10562-020-03429-z.

[47] W. Zhu, X. Chen, C. Li, Z. Liu, C. Liang, Manipulating morphology and surface engineering of spinel cobalt oxides to attain high catalytic performance for propane oxidation, J. Catal. 396 (2021) 179–191, https://doi.org/10.1016/j.jcat.2021.02.014.

[48] W. Zhang, Y. Zhou, M. Shamzhy, S. Molitorisová, M. Opanasenko, A. Giroir-Fendler, Total oxidation of toluene and propane over supported Co_3O_4 catalysts: Effect of structure/acidity of MWW zeolite and cobalt loading, ACS Appl. Mater. Interfaces 13 (2021) 15143–15158, https://doi.org/10.1021/acsami.0c21999.

[49] M. Wang, L. Qi, X. Li, Modulating defective oxygen of Co-based crystals by calcination temperature control for improving the catalytic removal of propane, CrystEngComm 24 (2022) 7902–7905, https://doi.org/10.1039/D2CE01257J.

[50] G. Chai, W. Zhang, L.F. Liotta, M. Li, Y. Guo, A. Giroir-Fendler, Total oxidation of propane over Co_3O_4-based catalysts: Elucidating the influence of Zr dopant, Appl.

Catal. B Environ. 298 (2021), 120606, https://doi.org/10.1016/j. apcatb.2021.120606.

[51] C.-F. Liu, L.-C. He, X.-F. Wang, J. Chen, J.-Q. Lu, M.-F. Luo, Tailoring Co_3O_4 active species to promote propane combustion over Co_3O_4/ZSM-5 catalyst, Mol. Catal. 524 (2022), 112297, https://doi.org/10.1016/j.mcat.2022.112297.

[52] K. Chen, W. Li, C. Zhu, L. Yuan, Construction of hollow cobalt tetroxide nanocages through the metal salt bifunctional etching strategy for catalytic oxidation of propane at ultrahigh space velocity, ACS Appl. Nano Mater. 5 (2022) 6575–6584, https://doi.org/10.1021/acsanm.2c00650.

[53] W. Zhang, C. Descorme, J.L. Valverde, A. Giroir-Fendler, Cu-Co mixed oxide catalysts for the total oxidation of toluene and propane, Catal. Today 384– 386 (2022) 238–245, https://doi.org/10.1016/j.cattod.2021.04.005.

[54] W. Zhang, C. Descorme, J.L. Valverde, A. Giroir-Fendler, Yttrium-modified Co_3O_4 as efficient catalysts for toluene and propane combustion: Effect of yttrium content, J. Hazard. Mater. 437 (2022), 129316, https://doi.org/10.1016/j. jhazmat.2022.129316.

[55] R.P. Marin, S.A. Kondrat, R.K. Pinnell, T.E. Davies, S. Golunski, J.K. Bartley, G. J. Hutchings, S.H. Taylor, Green preparation of transition metal oxide catalysts using supercritical CO_2 anti-solvent precipitation for the total oxidation of propane, Appl. Catal. B Environ. 140–141 (2013) 671–679, https://doi.org/ 10.1016/j.apcatb.2013.04.076.

[56] C. He, C. Ao, S. Ruan, K. Xu, L. Zhang, Catalytic combustion of propane over Zr-modified Co_3O_4 catalysts: An experimental and theoretical study, Colloids Surf. A Physicochem. Eng. Asp. 641 (2022), 128617, https://doi.org/10.1016/j. colsurfa.2022.128617.

[57] W. Zhu, X. Wang, C. Li, X. Chen, W. Li, Z. Liu, C. Liang, Defect engineering over Co_3O_4 catalyst for surface lattice oxygen activation and boosted propane total oxidation, J. Catal. 413 (2022) 150–162, https://doi.org/10.1016/j. jcat.2022.06.024.

[58] C. Li, X. Liu, H. Wang, Y. He, L. Song, Y. Deng, S. Cai, S. Li, Metal-organic framework derived hexagonal layered cobalt oxides with {112} facets and rich oxygen vacancies: High efficiency catalysts for total oxidation of propane, Adv. Powder Technol. 33 (2022), 103373, https://doi.org/10.1016/j.apt.2021.11.025.

[59] M. Zhang, X. Sui, X. Zhang, M. Niu, C. Li, H. Wan, Z.-A. Qiao, H. Xie, X. Li, Multi-defects engineering of $NiCo_2O_4$ for catalytic propane oxidation, Appl. Surf. Sci. 600 (2022), 154040, https://doi.org/10.1016/j.apsusc.2022.154040.

[60] K. Zha, S. Wu, Z. Zheng, Z. Huang, H. Xu, W. Shen, Insights into boosting SO_2 tolerance for catalytic oxidation of propane over Fe_2O_3-promoted Co_3O_4/ halloysite catalysts, Ind. Eng. Chem. Res. 61 (2022) 12482–12492, https://doi. org/10.1021/acs.iecr.2c01902.

[61] E. Wu, D. Lin, Y. Chen, X. Feng, K. Niu, Y. Luo, B. Huang, J. Qiu, Q. Qian, Q. Chen, N-doped CoAl oxides from hydrotalcites with enhanced oxygen vacancies for excellent low-temperature propane oxidation, J. Environ. Sci. 116 (2022) 79–89, https://doi.org/10.1016/j.jes.2021.07.003.

[62] G. Li, Z. Shui, X. Duan, H. Yang, Z. Zhao, T. Zhao, Z. Zhang, G. Jiang, H. Ren, J. Cheng, Z. Hao, Unveiling the balance between catalytic activity and water resistance over Co_3O_4 catalysts for propane oxidation: The role of crystal facet and oxygen vacancy, ACS Catal. (2022) 237–247, https://doi.org/10.1021/ acscatal.2c05640.

[63] L. Sun, X. Liang, H. Liu, H. Cao, X. Liu, Y. Jin, X. Li, S. Chen, X. Wu, Activation of Co-O bond in (110) facet exposed Co_3O_4 by Cu doping for the boost of propane catalytic oxidation, J. Hazard. Mater. 452 (2023), 131319, https://doi.org/ 10.1016/j.jhazmat.2023.131319.

[64] G. Salek, P. Alphonse, P. Dufour, S. Guillemet-Fritsch, C. Tenailleau, Low-temperature carbon monoxide and propane total oxidation by nanocrystalline cobalt oxides, Appl. Catal. B Environ. 147 (2014) 1–7, https://doi.org/10.1016/j. apcatb.2013.08.015.

[65] Z. Ren, Z. Wu, W. Song, W. Xiao, Y. Guo, J. Ding, S.L. Suib, P.-X. Gao, Low temperature propane oxidation over Co_3O_4 based nano-array catalysts: Ni dopant effect, reaction mechanism and structural stability, Appl. Catal. B Environ. 180 (2016) 150–160, https://doi.org/10.1016/j.apcatb.2015.04.021.

[66] M.S.L. Aparicio, I.D. Lick, Total oxidation of propane and naphthalene from emission sources with supported cobalt catalysts, React. Kinet. Mech. Catal. 119 (2016) 469–479, https://doi.org/10.1007/s11144-016-1052-3.

[67] W. Zhang, L. Hu, F. Wu, J. Li, Decreasing Co_3O_4 particle sizes by ammonia-etching and catalytic oxidation of propane, Catal. Lett. 147 (2017) 407–415, https://doi.org/10.1007/s10562-016-1956-6.

[68] W. Zhao, S. Ruan, Q. Sian, B. Feng, C. Ao, L. Wang, F. Liu, L. Zhang, Abatement of n-butane by catalytic combustion over Co-ZSM-5 catalysts, Energy Fuels 34 (2020) 12880–12890, https://doi.org/10.1021/acs.energyfuels.0c02717.

[69] Z. Hu, Z. Tang, T. Zhang, X. Yong, R. Mi, D. Li, X. Yang, R.T. Yang, Synergism between manganese and cobalt on Mn-Co oxides for the catalytic combustion of VOCs: A combined kinetics and diffuse reflectance infrared Fourier transform spectroscopy study, Ind. Eng. Chem. Res. 61 (2022) 4803–4815, https://doi.org/ 10.1021/acs.iecr.1c05077.

[70] C.Y. Ma, Z. Mu, J.J. Li, Y.G. Jin, J. Cheng, G.Q. Lu, Z.P. Hao, S.Z. Qiao, Mesoporous Co_3O_4 and Au/Co_3O_4 Catalysts for low-temperature oxidation of trace ethylene, J. Am. Chem. Soc. 132 (2010) 2608–2613, https://doi.org/ 10.1021/ja906274t.

[71] W. Li, Z. Zhang, J. Wang, W. Qiao, D. Long, L. Ling, Low temperature catalytic combustion of ethylene over cobalt oxide supported mesoporous carbon spheres, Chem. Eng. J. 293 (2016) 243–251, https://doi.org/10.1016/j.cej.2016.02.089.

[72] L.F.F. Liotta, M. Ousmane, G. Di Carlo, G. Pantaleo, G. Deganello, G. Marcì, L. Retailleau, A. Giroir-Fendler, Total oxidation of propene at low temperature over Co_3O_4–CeO_2 mixed oxides: Role of surface oxygen vacancies and bulk

[73] J. Bao, H. Chen, S. Yang, P. Zhang, Mechanochemical redox-based synthesis of highly porous $Co_xMn_{1-x}O_y$ catalysts for total oxidation, Chin. J. Catal. 41 (2020) 1846–1854, https://doi.org/10.1016/S1872-2067(20)63635-X.

[74] Q. Li, N. Luo, D. Xia, P. Huang, X. Liu, T. Odoom-Wubah, J. Huang, G. Chai, D. Sun, Q. Li, Interfacial effects in CuO/Co_3O_4 heterostructures enhance benzene catalytic oxidation performance, Environ. Sci. Nano. 9 (2022) 781–796, https:// doi.org/10.1039/D1EN01044A.

[75] Y. Shen, J. Deng, S. Impeng, S. Li, T. Yan, J. Zhang, L. Shi, D. Zhang, Boosting toluene combustion by engineering Co–O strength in cobalt oxide catalysts, Environ. Sci. Technol. 54 (2020) 10342–10350, https://doi.org/10.1021/acs. est.0c02680.

[76] Z. Song, M. Zhao, Y. Mao, X. Zhang, J. Luo, B. Liu, H. Lu, W. Liu, Y. Xing, X. Zhu, Turning the structural properties and redox ability of Co-La catalyst in the catalytic oxidation of toluene, Sep. Purif. Technol. 274 (2021), 119025, https:// doi.org/10.1016/j.seppur.2021.119025.

[77] Y. Guo, M. Wen, S. Song, Q. Liu, G. Li, T. An, Enhanced catalytic elimination of typical VOCs over $ZnCoO_x$ catalyst derived from in situ pyrolysis of ZnCo bimetallic zeolitic imidazolate frameworks, Appl. Catal. B Environ. 308 (2022), 121212, https://doi.org/10.1016/j.apcatb.2022.121212.

[78] W. Han, F. Dong, W. Han, J. Yao, Y. Meng, Z. Tang, A new strategy for designing highly efficient Co_3O_4 catalyst with the molecular space configurations for toluene catalytic combustion, Chem. Eng. J. 435 (2022), 134953, https://doi. org/10.1016/j.cej.2022.134953.

[79] J. Lei, S. Wang, J. Li, Y. Xu, S. Li, Different effect of Y (Y = Cu, Mn, Fe, Ni) doping on Co_3O_4 derived from Co-MOF for toluene catalytic destruction, Chem. Eng. Sci. 251 (2022), 117436, https://doi.org/10.1016/j.ces.2022.117436.

[80] S. Zhao, T. Li, J. Lin, P. Wu, Y. Li, A. Li, T. Chen, Y. Zhao, G. Chen, L. Yang, Y. Meng, X. Jin, Y. Qiu, D. Ye, Engineering Co^{3+}-rich crystal planes on Co_3O_4 hexagonal nanosheets for CO and hydrocarbons oxidation with enhanced catalytic activity and water resistance, Chem. Eng. J. 420 (2021), 130448, https://doi.org/10.1016/j.cej.2021.130448.

[81] J. Zhong, Y. Zeng, D. Chen, S. Mo, M. Zhang, M. Fu, J. Wu, Z. Su, P. Chen, D. Ye, Toluene oxidation over Co^{3+}-rich spinel Co_3O_4: Evaluation of chemical and by-product species identified by in situ DRIFTS combined with PTR-TOF-MS, J. Hazard. Mater. 386 (2020), 121957, https://doi.org/10.1016/j. jhazmat.2019.121957.

[82] Y. Ma, L. Wang, J. Ma, H. Wang, C. Zhang, H. Deng, H. He, Investigation into the Enhanced catalytic oxidation of o-xylene over MOF-derived Co_3O_4 with different shapes: The role of surface twofold-coordinate lattice oxygen (O 2f), ACS Catal. 11 (2021) 6614–6625, https://doi.org/10.1021/acscatal.1c01116.

[83] Y. Ma, L. Wang, J. Ma, F. Liu, H. Einaga, H. He, Improved and reduced performance of Cu- and Ni-Substituted Co_3O_4 catalysts with varying Co_{Oh}/Co_{Td} and Co^{3+}/Co^{2+} ratios for the complete catalytic oxidation of VOCs, Environ. Sci. Technol. 56 (2022) 9751–9761, https://doi.org/10.1021/acs.est.2c02450.

[84] Z. Jiang, X. Feng, J. Deng, C. He, M. Douthwaite, Y. Yu, J. Liu, Z. Hao, Z. Zhao, Atomic-scale insights into the low-temperature oxidation of methanol over a single-atom Pt_1-Co_3O_4 catalyst, Adv. Funct. Mater. 29 (2019) 1–10, https://doi. org/10.1002/adfm.201902041.

[85] L. Bai, F. Wyrwalski, M. Safariamin, R. Bleta, J.F. Lamonier, C. Przybylski, E. Monflier, A. Ponchel, Cyclodextrin-cobalt (II) molecule-ion pairs as precursors to active $Co_3O_4/ZrO2$ catalysts for the complete oxidation of formaldehyde: Influence of the cobalt source, J. Catal. 341 (2016) 191–204, https://doi.org/ 10.1016/j.jcat.2016.07.006.

[86] J. Deng, W. Song, L. Chen, L. Wang, M. Jing, Y. Ren, Z. Zhao, J. Liu, The effect of oxygen vacancies and water on HCHO catalytic oxidation over Co_3O_4 catalyst: A combination of density functional theory and microkinetic study, Chem. Eng. J. 355 (2019) 540–550, https://doi.org/10.1016/j.cej.2018.08.195.

[87] R. Li, Y. Huang, D. Zhu, W. Ho, J. Cao, S. Lee, Improved oxygen activation over a carbon/Co_3O_4 nanocomposite for efficient catalytic oxidation of formaldehyde at room temperature, Environ. Sci. Technol. 55 (2021) 4054–4063, https://doi.org/ 10.1021/acs.est.1c00490.

[88] H. Xie, H. Lan, X. Tan, W. Wang, L. Yan, X. Liu, G. Zhou, High-efficient oxidation removal of ethanol from air over ordered mesoporous $Co_3O_4/KIT-6$ catalyst, J. Environ. Chem. Eng. 7 (2019), 103480, https://doi.org/10.1016/j. jece.2019.103480.

[89] Q. Zhao, Q. Liu, Y. Zheng, R. Han, C. Song, N. Ji, D. Ma, Enhanced catalytic performance for volatile organic compound oxidation over in-situ growth of MnO_x on Co_3O_4 nanowire, Chemosphere 244 (2020) 125532, https://doi.org/ 10.1016/j.chemosphere.2019.125532.

[90] S. Dissanayake, N. Wasalathanthri, A. Shirazi Amin, J. He, S. Poges, D. Rathnayake, S.L. Suib, Mesoporous Co_3O_4 catalysts for VOC elimination: Oxidation of 2-propanol, Appl. Catal. A Gen. 590 (2020), 117366, https://doi. org/10.1016/j.apcata.2019.117366.

[91] M. Konsolakis, S.A.C. Carabineiro, G.E. Marnellos, M.F. Asad, O.S.G.P. Soares, M. F.R. Pereira, J.J.M. Órfão, J.L. Figueiredo, Effect of cobalt loading on the solid state properties and ethyl acetate oxidation performance of cobalt-cerium mixed oxides, J. Colloid Interface Sci. 496 (2017) 141–149, https://doi.org/10.1016/j. jcis.2017.02.014.

[92] Y. Zhang, Q. Zhao, C. Shan, S. Lu, Y. Su, R. Han, C. Song, N. Ji, D. Ma, Q. Liu, Enhanced acetone oxidation over the CeO_2/Co_3O_4 catalyst derived from metal–organic frameworks, ACS Appl. Mater. Interfaces 12 (2020) 28139–28147, https://doi.org/10.1021/acsami.0c04904.

[93] L. Zhang, S. Huang, W. Deng, D. Yang, Q. Tang, S. Zhu, L. Guo, Dichloromethane catalytic combustion over Co_3O_4 catalysts supported on MFI type zeolites,

Microporous Mesoporous Mater. 312 (2021), 110599, https://doi.org/10.1016/j.micromeso.2020.110599.

[94] Z. Boukha, J. González-Prior, B. de Rivas, J.R. González-Velasco, R. López-Fonseca, J.I. Gutiérrez-Ortiz, Synthesis, characterisation and behaviour of Co/hydroxyapatite catalysts in the oxidation of 1,2-dichloroethane, Appl. Catal. B Environ. 190 (2016) 125–136, https://doi.org/10.1016/j.apcatb.2016.03.005.

[95] C. Wang, C. Zhang, W. Hua, Y. Guo, G. Lu, S. Gil, A. Giroir-Fendler, Catalytic oxidation of vinyl chloride emissions over Co-Ce composite oxide catalysts, Chem. Eng. J. 315 (2017) 392–402, https://doi.org/10.1016/j.cej.2017.01.007.

[96] H. Liu, J. Yang, Y. Jia, Z. Wang, M. Jiang, K. Shen, H. Zhao, Y. Guo, Y. Guo, L. Wang, S. Dai, W. Zhan, Significant improvement of catalytic performance for chlorinated volatile organic compound oxidation over RuO_x supported on acid-etched Co_3O_4, Environ. Sci. Technol. 55 (2021) 10734–10743, https://doi.org/10.1021/acs.est.1c02970.

[97] J. Mei, W. Huang, Z. Qu, X. Hu, N. Yan, Catalytic oxidation of dibromomethane over Ti-modified Co_3O_4 catalysts: Structure, activity and mechanism, J. Colloid Interface Sci. 505 (2017) 870–883, https://doi.org/10.1016/j.jcis.2017.06.077.

[98] J. Mei, Z. Qu, S. Zhao, X. Hu, H. Xu, N. Yan, Promoting effect of Mn and Ti on the structure and performance of Co_3O_4 catalysts for oxidation of dibromomethane, J. Ind. Eng. Chem. 57 (2018) 208–215, https://doi.org/10.1016/j.jiec.2017.08.025.

[99] S. Li, D. Wang, X. Wu, Y. Chen, Recent advance on VOCs oxidation over layered double hydroxides derived mixed metal oxides, Chin. J. Catal. 41 (2020) 550–560, https://doi.org/10.1016/S1872-2067(19)63446-7.

[100] T. Lu, F. Su, Q. Zhao, J. Li, C. Zhang, R. Zhang, P. Liu, Catalytic oxidation of volatile organic compounds over manganese-based oxide catalysts: Performance, deactivation and future opportunities, Sep. Purif. Technol. 296 (2022), 121436, https://doi.org/10.1016/j.seppur.2022.121436.

[101] Y. Zheng, K. Fu, Z. Yu, Y. Su, R. Han, Q. Liu, Oxygen vacancies in a catalyst for VOCs oxidation: synthesis, characterization, and catalytic effects, J. Mater. Chem. A 10 (2022) 14171–14186, https://doi.org/10.1039/d2ta03180a.

[102] C.W. Tang, C. Bin Wang, S.H. Chien, Characterization of cobalt oxides studied by FT-IR, Raman, TPR and TG-MS, Thermochim. Acta 473 (2008) 68–73, https://doi.org/10.1016/j.tca.2008.04.015.

[103] X. Wang, Y. Liu, T. Zhang, Y. Luo, Z. Lan, K. Zhang, J. Zuo, L. Jiang, R. Wang, Geometrical-site-dependent catalytic activity of ordered mesoporous co-based spinel for benzene oxidation: in situ DRIFTS study coupled with Raman and XAFS spectroscopy, ACS Catal. 7 (2017) 1626–1636, https://doi.org/10.1021/acscatal.6b03547.

[104] P. Atkins, T. Overton, J. Rourke, M. Weller, F. Armstrong. Shriver and Atkins' Inorganic Chemistry, Fifth.,, Oxford University Press,, USA, New York, 2009. ⟨http://www.amazon.co.uk/Shriver-Atkins-Inorganic-Chemistry-Peter/dp/0199236178⟩.

[105] X. Xie, Y. Li, Z.-Q. Liu, M. Haruta, W. Shen, Low-temperature oxidation of CO catalysed by Co_3O_4 nanorods, Nature 458 (2009) 746–749, https://doi.org/10.1038/nature07877.

[106] Z. Chen, S. Wang, W. Liu, X. Gao, D. Gao, M. Wang, S. Wang, Morphology-dependent performance of Co_3O_4 via facile and controllable synthesis for methane combustion, Appl. Catal. A Gen. 525 (2016) 94–102, https://doi.org/10.1016/j.apcata.2016.07.009.

[107] W. Liu, R. Liu, X. Zhang, Controllable synthesis of 3D hierarchical Co_3O_4 catalysts and their excellent catalytic performance for toluene combustion, Appl. Surf. Sci. 507 (2020), 145174, https://doi.org/10.1016/j.apsusc.2019.145174.

[108] W. Liu, R. Liu, H. Zhang, Q. Jin, Z. Song, X. Zhang, Fabrication of Co_3O_4 nanospheres and their catalytic performances for toluene oxidation: The distinct effects of morphology and oxygen species, Appl. Catal. A Gen. 597 (2020), 117539, https://doi.org/10.1016/j.apcata.2020.117539.

[109] Y. Liu, H. Dai, J. Deng, S. Xie, H. Yang, W. Tan, W. Han, Y. Jiang, G. Guo, Abatement of various types of VOCs by adsorption/catalytic oxidation: A review, Chem. Eng. J. 370 (2019) 1128–1153, https://doi.org/10.1016/j.cej.2019.03.232.

[110] Y. Liu, H. Dai, J. Deng, S. Xie, H. Yang, W. Tan, W. Han, Y. Jiang, G. Guo, Mesoporous Co_3O_4-supported gold nanocatalysts: Highly active for the oxidation of carbon monoxide, benzene, toluene, and o-xylene, J. Catal. 309 (2014) 408–418, https://doi.org/10.1016/j.jcat.2013.10.019.

[111] Z. Fan, Z. Zhang, W. Fang, X. Yao, G. Zou, W. Shangguan, Low-temperature catalytic oxidation of formaldehyde over Co_3O_4 catalysts prepared using various precipitants, Chin. J. Catal. 37 (2016) 947–954, https://doi.org/10.1016/S1872-2067(15)61086-5.

[112] C. Cao, L. Xing, Y. Yang, Y. Tian, T. Ding, J. Zhang, T. Hu, L. Zheng, X. Li, Diesel soot elimination over potassium-promoted Co_3O_4 nanowires monolithic catalysts under gravitation contact mode, Appl. Catal. B Environ. 218 (2017) 32–45, https://doi.org/10.1016/j.apcatb.2017.06.035.

[113] M. Li, F. Bi, Y. Xu, P. Hao, K. Xiang, Y. Zhang, S. Chen, J. Guo, X. Guo, W. Ding, Effect of residual chlorine on the catalytic performance of Co_3O_4 for CO oxidation, ACS Catal. 9 (2019) 11676–11684, https://doi.org/10.1021/acscatal.9b03797.